POLITECNICO DI TORINO

Corso di Laurea Magistrale

In Ingegneria Energetica e Nucleare

Tesi di Laurea Magistrale

Modeling of an industrial-size AEC and estimation of the purity of the product gas

Relatore:
Prof. Massimo Santarelli
Co-relatore:
Dott.Paolo Marocco
Tutor aziendale:
Ing. Luca Baldini

Candidata:
Ilenia Cicciò

A.A. 2018/2019

Table of Contents

Nomenclature

A_{el}	Geometrical electrode area	m^2
A_{GL}^{j}	Gas-liquid interfacial area in compartment j	m^2
A_{sep}	Separator area	m^2
c_i^{mix}	Mixer outlet concentration of component i	mol m^{-3}
$c_{in,i}^{j}$	Inlet concentration of component i in compartment j	mol m^{-3}
$c_{in,i}^{j}$	Outlet concentration of component i in compartment j	mol m^{-3}
$c_i^{*,j}$	Equilibrium concentration of component i in compartment j	mol m^{-3}
d_b^j	Gas bubble diameter in compartment j	M
d_{sep}	Sepatator thickness	M
$D_{i,k}$	Binary diffusion coefficient of component i in electrolyte solution k	$m^2 s^{-1}$
$D_{i,k}^{eff}$	Effective diffusion coefficient of component i in the separator	$m^2 s^{-1}$
V	Standard electrode potential	V
F	Faraday constant	96.485 C mol^{-1}
$f_{G,i}$	Gas evolution efficiency of component i	1
g	Gravity	9.823 m s^{-2}
H_i	Henry coefficient of component i	Atm
J	Current density	A m^{-2}
$k_{L,i}^{j}$	Mass transfer coefficient of component i in compartment j	m s^{-1}
M_{KOH}	Molar mass of potassium hydroxide	0.0561056 kg mol^{-1}
M_{H_2O}	Molar mass of water	0.018 kg mol^{-1}
m_{KOH}	Molality of potassium hydroxide solution	mol kg^{-1}
$N_{cross,i}$	Flux density through the separator of component i	mol $m^{-2}s^{-1}$
$N_{phys,i}^{j}$	De-or absorption flux density of component i in compartment j	mol $m^{-2}s^{-1}$
$n_{R,i}^{\cdot j}$	Molar reaction flow rate of component i in compartment j	mol s^{-1}
p^0	Applied system pressure	Pa
p^j	Absolute pressure in compartment j	Pa
p_{H_2O}	Partial pressure of water	Pa
$p_{in,i}^{j}$	Inlet partial pressure of component i in compartment j	Pa
$p_{out,i}^{j}$	Outlet partial pressure of component i in compartment j	Pa
R	Universal gas constant	8.314 J $mol^{-1}K^{-1}$

Re^j	Reynolds number in compartment j	1
S_b^j	Single gas bubble surface area in compartment j	m^2
Sc_i	Schmidt number of component i	1
Sh_i^j	Sherwood number of component in compartment j	1
Sc_i	Schmidt number of component i	1
Sh_i^j	Sherwood number of component in compartment j	1
T	Temperature	K
u_b^j	Single bubble rise velocity in compartment j	$m\ s^{-1}$
u_{sw}^j	Bubble swarm rise velocity in compartment j	$m\ s^{-1}$
V_b^j	Single gas bubble volume in compartment j	m^3
V_{gas}^j	Total gas volume in compartment j	m^3
V_{hcell}	Total half cell volume	m^3
$\dot{V}_G^j$	Volumetric gas flow rate in compartment j	$m^3\ s^{-1}$
$\dot{V}_L^j$	Volumetric liquid electrolyte flow rate in compartment j	$m^3\ s^{-1}$
$\dot{V}_L^{mix}$	Outlet volumetric liquid electrolyte flow rate of mixer	$m^3\ s^{-1}$
w_{KOH}	Mass fraction of potassium hydroxide in electrolyte solution	1
$x_{out,i}^j$	Outlet mole fraction of component i in compartment j	1
z	Number of transferred eletrons in electrode reaction	1
β^j	Contact angle of gas – solid interface in compartment j	1
Γ	Surface tension	$N\ m^{-1}$
E	Porosity	1
ε_g^j	Gas voidage in compartment j	1
$\varepsilon_{g,out}^j$	Outlet gas voidage in compartment j	1
η_L	Electrolyte viscosity	Pa s
Θ	Temperature	°C
k_L	Electrical conductivity of electrolyte solution	$S\ m^{-1}$
ν_i^j	Stoichiometric coefficient of component i in compartment j	1
ρ_G^j	Gaseous density in compartment j	$kg\ m^{-3}$
ρ_L	Electrolyte density	$kg\ m^{-3}$
τ	Tortuosity	1

Abbrevation

Ano	anode
Cat	cathode
CFD	computational fluid dynamics
CSTR	continuous stirred- tank reactor
DC	direct current
PEM	proton exchange membrane/ polymer exchange membrane

Figure index

Abstract

Nowadays one of the most important global problems is to research and to develop an electric energy production environmentally sustainable.

In fact, all recent studies carry out the unsustainability of keeping the current power generations, carbon-based, this involves the imperative for the electricity production sector to evolve and develop new clean sources of energy and techniques. At the moment, new technologies present many disadvantages such as the investment costs and the efficiencies of the plants' work. For this reason a lot of strength are spent by governments and companies to encourage and to develop the current technologies. Another important fact is that electrical energy produced by renewable sources has to be fixed with the users' demand: there are many surpluses of energy produced when the requirement is low and the energy is lost. In order to minimize the issue of energy, it can be stored in many different ways and when there is high users demand it can be used to provide the request. But the current technologies to stock energy lack good performances.

One of the brightest developing in the storage energy industry is Hydrogen accumulation technologies, the purpose of this study. Due to the mixed work of Fuel Cells and the Electrolyzers and using the water electrolysis, the surplus energy can be stored in the form of hydrogen and it can be converted

into power when it is needed. This method of implementation is called Power to Power (P2P), its advantage is to produce electric energy in the situation of an isolated or remote grid. But, as mentioned above, this type of system needs optimization in order to improve its performance.

The product gas of Alkaline Electrolyzer are Oxygen and Hydrogen: both theoretically should have high purity, but in the practice, the level of this purity depends on the operational conditions.

The estimation of the outlet variation hydrogen purity is the goal of this research. The outlet purity depends on the border condition features such as the temperature, the inlet power, the mass flow rate, and the KOH concentration. This was achieved building a theoretical model and running several tests performed to the company.

This investigation revealed that gas purity in alkaline water electrolyzer is directly related to the inlet power, higher levels of cleanness are reached by increasing the input power.

This study was split into several parts. Starting from the Power to Power concept at first is explained how the development of energetic technology is important, above all hydrogen topic. Then how to store energy and how to use hydrogen in order to obtain power.

After general paths, the company's plant is described in detail, in particular, is explained Self 25, the company's alkaline electrolyzer, with his components. The process modeling of an alkaline water electrolyzer consists of an accurate engineering analysis, that is the principal body of this thesis.

The last two chapters shown the construction of the model with the results and the company's test performed respectively.

The study ends with a comparison between model and tests results, in order to understand from which parameter the Hydrogen purity depends and how to optimize an alkaline electrolyzer for better applications.

1 General Concepts

The theory, which is based the research on, was presented in the following chapter. Coming forward the definition of power to power system and the role of the hydrogen in the situations off-grid and isolated micro-grid both.

Then, every reader will own the knowledge needed to understand the aim of this research and the prominence of applying the studied technology nowadays, such as implementing it for the remote locations cut of the power network, in order to drop the carbon dioxide emissions down.

1.1 P2P concept

The worldwide energy industry development is to ensure the requiring power for any industrial and civil applications. One of the main challenges to reach the world's energy demand is to improve the currents energy storage's systems performances [1].

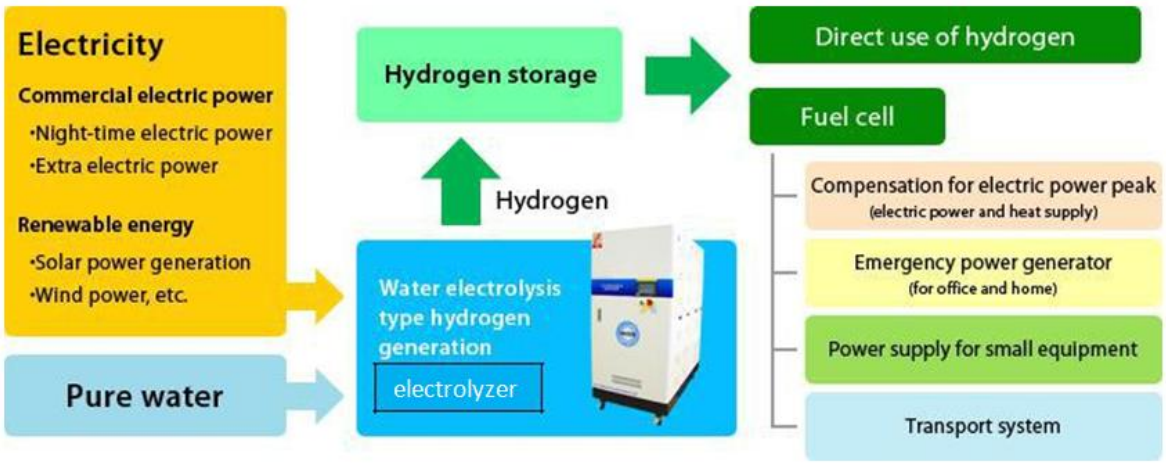

Fig. 1.1.1: schematic application of electrolyzer technology

The power-to-power (P2P) concept was created in order to reuse the energy surplus occurred in the device, the exceeded power will be stored for the power production. The main technology's limit is to stock the energy because it's not possible directly storing the energy produced. In fact, the energy needs to be converted into a storable form. Several approaches were developed for energy storage depending on the production's method.

The work in this thesis was focused on Hydrogen storage technologies, developed on electrolyzer devices, combined with a fuel cell to reuse the supply energy.

Fuel Cell and Hydrogen (FCH) technologies (better explained in the following paragraphs) holds great promise in the energy's production and management; thus, to meet the European environmental and economic challenges in the energy industry [2] such as:

- Help to fight carbon dioxide emissions
- Reduce dependence on mainly imported hydrocarbons
- Contribute to economic growth and create employment

Recent studies proved that hydrogen, applied to stock electricity, sustainable biofuels, and natural gas, will gradually become a much more significant component of the European energy industry. Nowadays, fuel cells are the most efficient means of converting various fuels, especially hydrogen, cleaner, more efficient, more reliable power and heat for a wide range of specific applications; these include portable devices, combined heat, and power (CHP), stationary power generation and road and non-road transport. A recent report has concluded that hydrogen, as an energy vector and storage medium, will substantially reduce the need for ever-greater quantities of renewable electricity, biofuels, and bio-energy necessary to create a sustainable low-carbon energy system after 2030. Furthermore, independent near to midterm market projections worldwide indicate substantial growth in the sector with positive impacts on direct industry and associated supply-chain jobs [2].

1.2 H_2-battery storage in situation off-grid or isolated micro-grid

In view of high renewable electricity targets in some regions, electrolysis is seen by many stakeholders as an element to address the potentially increasing challenges of integrating intermittent renewables energies. Electrolysers would operate when electricity generation is in excess of demand, or available at very low prices (e.g., during periods of high solar irradiation), thereby avoiding or reducing the need to curtail renewable electricity generation [1].

The produced hydrogen could then be stored locally, or fed into the natural gas infrastructure, and be used in transport, heating or for re-electrification in power plants. Hydrogen production via electrolysis is often broadly classed as energy storage, irrespective of the final use of the hydrogen. As no formal definition exists, we have chosen a comparatively narrow definition of energy storage, only covering those applications where the electrolyzer usage profile is mainly designed to shift energy system loads in time, often across markets. So, for instance, an electrolyzer that only operated on excess renewable electricity would be considered energy storage, whereas one at a refueling station nominally operating 8,760 hours per year would not [1]. Because they will need to respond to intermittent and fluctuating renewable power generation, the ability to operate dynamically is often mentioned as a key requirement for electrolyzers to play the role above in high renewables energy systems. A number of electrolyzer operating strategies can be used to help balance supply and demand. Different strategies, which may be combined, have been suggested by stakeholders:

- Limiting operation to times of excess or low-cost renewable power generation, which is expected to result in load factors of a maximum between 2,000 and 4,000 hours per year in 2050. This would require a system design optimized for efficient standby modes and would keep low capital cost over high efficiency.
- Taking part in the markets for operational reserves (i.e., load shedding in case of grid incidents). This would require a system design optimized for the quick response and start-up times.
- Taking advantage of highly fluctuating electricity prices. This would require a system design able to operate at a wide range of part loads, with the highest efficiency at low

part loads (operating at full load at suboptimal efficiency when electricity prices are low, operating at low part load with highest efficiency when electricity prices are high).

- Allowing flexibility on very constrained grids. In regions (such as islands) where high penetration of renewables has already been achieved, the use of hydrogen as an alternative energy vector to electricity may be beneficial. It is important to note that while these different operating strategies (and the system performance characteristics that they imply) are being looked into by stakeholders and tested at pilot and demonstration plants, the industry is currently rather uncertain as to which of the requirements will ultimately be valuable in a future energy market, and support of organizations like Fuel Cell and Hydrogen Joint Undertaking (FCHJU) could prove valuable in helping define these characteristics [3].

A possible power-to-power application is shown in the picture below and consists of coupling in a single machine an electrolyzer and a fuel cell. Power is provided by the electrical grid and/or by renewables to the load, and the surplus is used by the electrolyzer to store energy into pressurized hydrogen cylinders. The H2 then feeds the fuel cell and overcome the lack of power to the load when occurring.

This kind of technology is particularly effective for telecommunication systems to guarantee electrical power continuity all the time.

Fig. 1.2.1: electrolyzer operating scheme.

1.3 Hydrogen

Identifying and building a sustainable energy system are both critical issues for any modern society [4]. Ideally, the current energy system, based mostly on fossil fuels (which have limited supply and considerable negative environmental impact) would be replaced with a system based on a combination of renewable fuels. Hydrogen, as an energy carrier primarily derived from water, can address the issues of sustainability, environmental emissions, and energy security.

Hydrogen is the most abundant element in the universe, burns cleanly, producing only water and has the highest energy density per unit mass; this is why hydrogen is considered the most suitable to replace fossil fuels as the raw energy material for the industry.

However, hydrogen is not an energy source, only an energy carrier, and it is not freely available in nature (needs to be produced) either from water or other compounds. If it is produced from water, it costs more energy to produce it than could be recovered burning it.

This is why, ideally, a hydrogen cycle would include hydrogen produced by splitting water using electrolysis with solar energy and stored reversibly in a solid. Unfortunately, there are considerable difficulties associated with efficient hydrogen production, storage and use in fuel cells; among them, hydrogen storage for mobile applications is currently the most difficult obstacle [5]. Gasoline has a higher energy density (31.6 MJ/l) than compressed hydrogen (4.4 MJ/l) and liquid hydrogen (8.8 MJ/l). In addition, gasoline tank has extremely short filling time, is capable of providing energy at low temperatures and provides excellent control of energy discharge, allowing rapid acceleration, high sustained speed, and considerable range; these are the challenges that a successful hydrogen tank has to meet. Target requirements for a hydrogen tank require a gravimetric density of 7.5 wt. % and volumetric density of 70 g/l, operating temperature between 233 and 358K, the minimum delivery pressure of 12bar (1.2 Mpa) and fueling time of 3 minutes. In addition, the storage system should be safe, durable (1500 operational cycle life) and cost-effective. None of the existing systems meet these requirements yet. To put things in perspective in terms of mobility and industrial applications, figure 1 provides information on the energy content of hydrogen in comparison with gasoline. HHV and LHV indicate the Higher and Lower Heating Value of hydrogen. In order to achieve the hydrogen economy, there are some obstacles that need to be overcome to make hydrogen a viable energy carrier. They are characterized by four main aspects of hydrogen use and some of these will be addressed here:

- Production – since hydrogen needs to be produced (ideally from water) it is necessary to develop production methods that would consume the least amount of energy and be able to produce hydrogen renewably on a large scale.
- Storage – fuel needs to be easily stored to use and transport, where one of the main requirements is that hydrogen is readily available, which requires not only short charge/discharge times, but also excellent control of charge/discharge process coupled with sufficient energy and gravimetric/volumetric density.
- Power generation – once hydrogen is ready to be consumed, it is necessary to do so in the most effective way: the power generation system that consumes hydrogen needs to be both efficient and, for mobile application, lightweight.

- Safety – hydrogen use and storage comes with some risks (flammability) which necessitate certain precautions and safety measures; another related aspect is the environmental impact of the hydrogen cycle, which depends on the methods used for production, storage, and usage.

Since hydrogen is thought to be a renewable fuel for the future, it is only appropriate that, when we consider all the challenges associated with its production, storage, and use, we keep in mind that when we consider proposed systems, efficiency is only one of the factors that will determine the success of these systems. Other important aspects are durability, the stability of operation and safety, and these can, more than efficiency, determine the success or failure of any of the proposed solutions for a part of the hydrogen cycle [5].

1.3.1 Hydrogen production and application

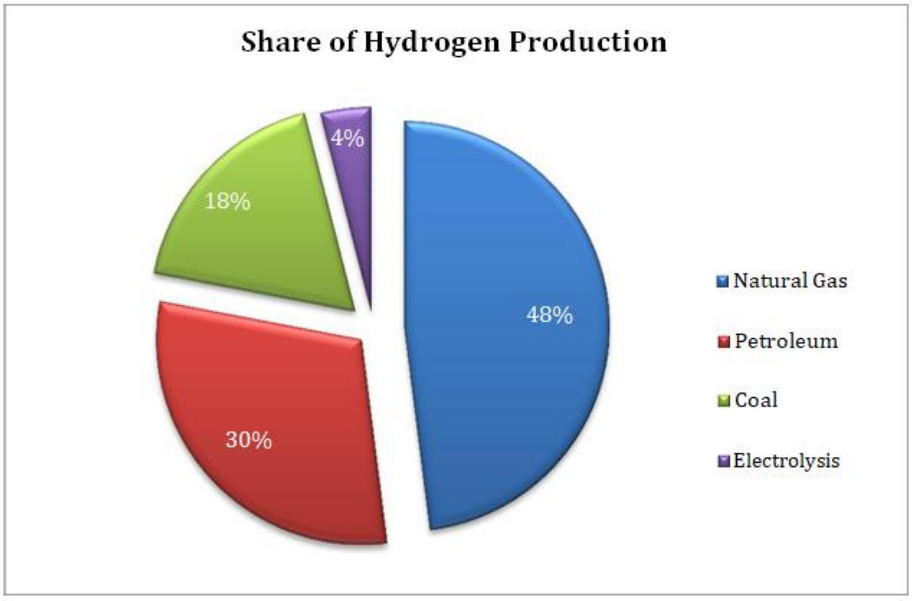

Fig. 1.3.1: Different ways for hydrogen production

There are several potential sources of hydrogen on our planet, although these are exclusively hydrogen compounds, necessitating extraction of hydrogen at an energy cost. The most abundant in the Earth is water; hydrogen can also be obtained from hydrocarbons, either fossil fuels or biomass. Figure 3 gives an overview of a share of hydrogen production; it can be seen that the majority of current production is by reforming of hydrocarbons while electrolysis contributes less than 5 %. While production from water is clean (given the electricity used is produced by emission-free methods) and renewable (with no CO_2 emissions) production from fossil fuels generates similar or even higher levels of CO_2 emissions as the burning of coal and gasoline. Hydrogen production from biomass is carbon neutral since plants and organisms used during the process sequester approximately the same amount of CO_2 during their growth as it is emitted during the process of extraction of hydrogen from them. However, their negative environmental impact is considerable due to the fact that they require large land surfaces to grow. Since we discuss hydrogen production from electrolysis at length later, we review other methods briefly.

Fossil Fuels

Fossil fuels are the dominant source of industrial hydrogen today. Hydrogen can be produced from natural gas with efficiency of around 80% and from other hydrocarbon sources with a varying degree of an efficiency. The most widely used method of hydrogen production today is steam reforming of methane or natural gas. At high temperatures (1000-1300K), water vapor reacts with methane to yield syngas (a mixture of hydrogen and carbon monoxide), which can be used to produce more hydrogen through reaction of water and carbon monoxide (also known as water gas shift reaction, performed around 400K). The drawback of this process is that it produces CO_2 waste [6]. Other methods of hydrogen production from fossil fuels are partial oxidation of hydrocarbons, which includes partial combustion of fuel-air mixture at high temperatures or in a presence of a catalyst, plasma reforming (Kvaerner process), which produces hydrogen and carbon black from hydrocarbons (no CO2 waste), and coal gasification, where coal is converted to syngas and methane.

Thermolysis

Water thermolysis is thermal dissociation of water, which occurs spontaneously around 2800K. Although this temperature is too high for practical applications, significant effort has been invested in research of catalysts to reduce water thermolysis temperature and make it an industrially viable process. The goal is to use water thermolysis either in solar concentrators or in nuclear power plants to produce hydrogen directly using thermal energy. Solar concentrators can produce very high temperatures (over 1800K) by concentrating sunlight using a system of mirrors. Next generation nuclear power plants will be operating at lower temperatures (1000-1300K), but it is hoped that new catalysts will make it possible to use them for direct hydrogen generation using water thermolysis.

Photocatalysis

Photocatalytic water splitting is a process of directly producing hydrogen using solar energy. It relies on the use of photocatalyst to capture the solar energy and use for water dissociation [7]. There are two principal types of catalysts: photoelectrochemical and photobiological.

Biohydrogen production

Biological H_2 production represents an effort to harness biological processes to generate hydrogen on the industrial scale. Although they have found no industrial application, there are a number of processes for conversion of biomass and waste streams into biohydrogen. Some of them are the same as the ones described above for fossil fuels, except they use biomass in place of fossil fuel (biomass gasification, steam reforming), while others use biological conversion of solar energy [8]. Biological conversion is a process where biological organisms (usual plants) convert sunlight into hydrogen through their metabolic processes [9].

In spite of these many methods of hydrogen production, to this date, reforming and electrolysis remain commercially significant technologies.

2 Electro-Chemical Cells

The aim of this chapter is to explain the general basic theory about the topic studied on this thesis. In particular what electro-chemical cells are, why to use and the general path about PEMFC (Proton Exchange Membrane Fuel Cell) and AEC (Alkaline Electrolytic Cell).

2.1 Principles of electro-chemical cells

Chemical energy can be defined as the property of a stream of mass, characterized by the high value of the Gibbs free energy (or free enthalpy).

The Gibbs energy (also referred to as *G*) is the thermodynamic potential, that can be used to estimate the spontaneously of a process, that reaches the minimum when a system gains the chemical equilibrium at constant pressure and temperature. As such, a reduction in *G* is a necessary condition for the spontaneity of processes.

The classical way to take advantage of chemical energy in order to produce electrical power is:

- Produce heat at high temperature (thermo-chemical transformation)
- Produce mechanical power in a thermodynamic cycle fed by heat at high temperature (thermo-mechanical transformation)
- Produce electrical power in an alternator (electro-mechanical transformation)

Electro-chemical cells are able to directly converts chemical energy into electric one, ensuring low energy leaks then, the low value of Σ_{irr} (irreversibility) and high efficiencies (at least~ 0.7).

Furthermore, they also can be run in both directions: chemical to electric transformation $\Delta G<0$ (power production) or electrical to chemical transformation $\Delta G>0$ (chemical species production).

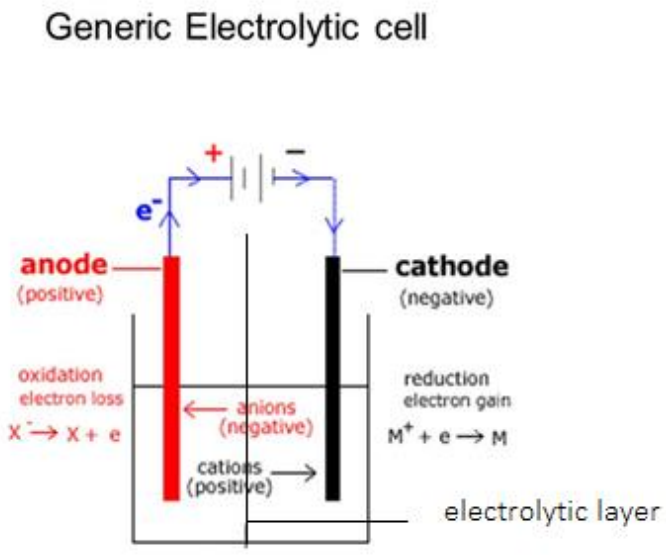

Fig. 2.1.1: Generic Electrolytic cell

The anode is the electrode where the reaction of oxidation occurs. It will be established the equilibrium.

$$R_1 \leftrightarrow O_x + e^-$$

The cathode is the electrode where the reaction of reduction occurs. It will be established the equilibrium.

$$R_2 + O_x + e^- \leftrightarrow P$$

At the end the global phenomena are:

$$R_1 + R_2 \longrightarrow P$$

Where R_1 and R_2 are generic reactants and P is the generic product.

The electrolytic layer physically separates the anode and the cathode. It should be characterized by a low molecular diffusivity, a low capability to conduct e^- and a high capability to conduct ions.

Even if there is no contact between the two reactants (thanks to electrolyte layer) the reaction occurs because the ions (oxidized form of reactant R_1) can go through the electrolyte and e^- can travel in an external circuit (since they cannot through the electrolyte, they will follow an alternative path).

Then, the ions carried out by the charge separation occurred in the reactions, produce electrical fields on both electrodes. Therefore, between the electrodes, a voltage differential ΔV grows.

By closing the external circuit, the equilibriums at the electrodes are broken and an electric current I is generated by e^- flow. The pressure of the current I flowing across a voltage gradient will generate electrical power W_{el}.

A galvanic cell is an electro-chemical cell where the external circuit is closed, in which the disequilibrium of reactants in terms of Gibbs free energy is directly transformed into electrical power ($\Delta G \rightarrow W_{el}$). The galvanic cells are of different types in the base of the ions that pass from the electrolytic layer: cationic electrolyte conductor of + ions (H^+), anionic electrolyte conductor of – ions (O^{2-}).

The only situation in which the cell is working in reversible conditions is when the circuit is open. If the circuit is open, no transport phenomena occur, and, as a consequence, there is no generation of entropy (reversible conditions).

The voltage measured across the cell in such a situation is called Open Circuit Voltage (OCV).

2.1.1 Electrolytic cells

An electrolytic cell is an electrochemical cell in which a not spontaneous reaction ($\Delta G>0$) is driven by electrical power: electrical energy is transformed into chemical energy associated to a chemical element/compound. ($W_{el} \rightarrow \Delta G$). The electrolytic cells are different because of the different ions passing through the electrolytic layer: cationic electrolyte (H^+), anionic electrolyte (O^{2-}), alkaline electrolyte (OH^-).

The electrochemical cells are divided into open and closed systems.

Open systems: the reaction takes place because reactants molecules are continuously supplied to the system in the form of a stream of mass coming from outside. Materials which the electrodes are made up do not participate in the reaction (they remain unchanged). These are the Fuel Cells.

Closed system: reaction is fed by molecules which are contained into the structure of the electrodes. Therefore, the material of the electrode participates to the reaction. No feeding from outside. These are the batteries.

Both of these systems can work in discharge regime (Fuel: $\Delta G<0$; Product: $W_{el}>0$), charge regime (fuel: $W_{el}<0$; Product: $\Delta G>0$).

2.2 Fuel Cells

Fuel cells are open electrochemical cells working in galvanic regime ($\Delta G<0$). Therefore, they consume the chemical energy contained in the reactants (H_2 and O_2) in order to produce electrical power.

Fuel cells are classified depending on the material composing of the electrolyte, which in turn determine the operational temperature range.

- 700°C/800°C: SOFC (Solid-Oxide Fuel Cell);
- 600°C/650°C: MSFC (Molten Salt Fuel Cell);
- 250°C: PAFC (Phosphoric Acid Fuel Cell);
- 50°C/80°C: PEMFC (Proton Exchange Membrane Fuel Cell);

AFC (Alkaline Fuel Cell);

DMFC (Direct Methanol Fuel Cell).

The PEMFC dominate the market in term of stability and costs

2.2.1 PEMFC

A Proton Exchange Membrane fuel cell delivers high-power density while providing low weight, cost, and volume.

Now we consider a single cell, it consists of:

- Positively charged electrode (cathode), where oxygen is reduced. At the cathode, oxygen reacts with protons (ions H^+) and e^- forming water and producing heat.
- Negatively charged electrode (anode), where hydrogen is oxidized. At the anode, hydrogen reacts delivering protons (ions H^+) and e^-.
- PEM electrolyte layer, which let ions H+ pass through it, while it is tight to molecules and e^-.
- GDL, gas diffusion layer, which is porous layers (Ɛ=0.3/0.8) electrically conductive, whose function is to transport the fuel/product from the fuel flow channels in the bipolar plates to the reaction side, and to electrically connect the electrodes with the external circuit.
- GASKET, which is needed to prevent gas/fluids leakages.
- BIPOLAR PLATE, which is responsible of delivering the fuels and removing the products through channels formed on its surface and to electronically connect cells in a series configuration.

The total reaction occurring in a PEMFC is:

$$H_2 + \frac{1}{2}O_2 \longrightarrow H_2O$$

where

$$OCV(T = 25°C; p = 1\ bar) = 1.23\ V$$

However, PEMFC usually works at different temperature and pressure:

$$OCV(T = 60°C; p = 1\ bar) = 1.18\ V$$

1.18 V is a very low value to produce a significant amount of power; therefore, there is the necessity to stack the cells in a series configuration. In the presence of a stack of cells, the produced power will be

$$W_{el} = n_c \times V_c \times I = n_c \times V_c \times i \times s$$

Each cell in the stack may be producing a different voltage wrt the others, because of the different thermodynamic condition.

Efficiency

Electrical efficiency is strictly dependent on the voltage:

$$\eta_{el}(i) = k * V_c(i)$$

$$W_{el}(i) = (n_c * S * V_c) * i$$

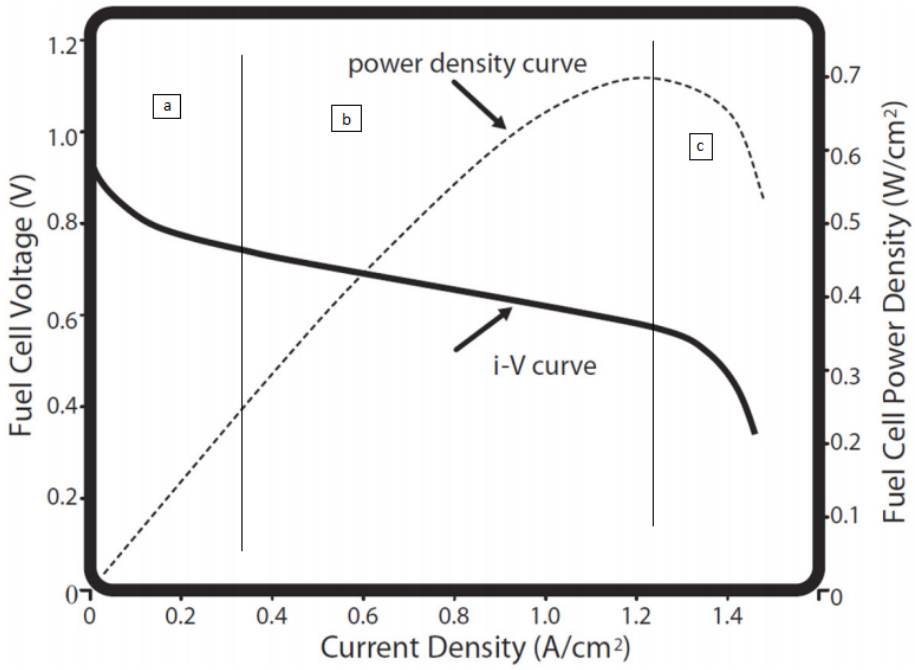

Fig. 2.2.1: Fuel Cell Voltage and Power Density on Current Density

In the following graph i-V curve and power density curve are represented and as you can see there are three parts in which you can operate:

a) If we want to operate at high efficiency, in order to simultaneously have acceptable electrical power, the system has to be oversized (high S, high n_c) which involve very high CAPEX (cost of investment). However, during the operation high value of efficiency guarantees low OPEX (cost of operation).
b) This is the most interesting part in which operate. This because the efficiency is still high and simultaneously, I is high enough to provide a significant amount of power.
c) If we want to operate at high electrical power, there is no need to oversize the system, because it will work with low efficiencies. This configuration involves low OPEX but very high CAPEX. Actually, it is totally useless to operate in this zone, because it would provide the same electrical power that could be achieved before the maximum.

Application

PEMFC are mainly observed to:

1. Automotive
2. Micro CHP (residential) →0.5kW
3. Distributed CHP (combined heat and power or cogeneration) →10/100 kW

Is clear that fuel cells alone are not able to produce electrical power. In order to achieve this task, fuel cells require a certain number of auxiliary systems. All the auxiliaries working alongside the PEMFC are called Balance of Plant (BOP):

- Fuel processing→ PEMFC has to be supplied with pure hydrogen to avoid catalyst poisoning. However, pure hydrogen does not exist in nature, but it has to be produced. For this reason, a fuel processing unit is mandatory.
- Thermal management→ PEMFC has to be cooled down continuously to avoid membrane drying. For this reason, a recirculation system for the cooling fluid is mandatory. Such a system is composed of pumps, pipes, valves and heat exchanger for heat recovery.

- Power conditioning→ DC/DC and DC/AC transformation and connection to the grid

2.3 Electrolyzers

Electrolyzers are open electrochemical cells working in reverse operation (W_{el}→$\Delta G>0$).

The polarization curve expresses the relation between the potential across the electrodes (V_c) and the density current flowing through the cell. Of course, such a relation will depend on the OCV and on all the overpotential that may take place in the cell.

$$V_c(T,p,i) = OCV(T,p) \pm Activation\ losses \pm Ohmic\ losses \pm Diffusion\ losses$$

The polarization curve for a specific electrolyzer is quite symmetric to the polarization curve for the associated fuel cell, but not exactly symmetric. This happens because there are different rate of reaction and so require different catalysts to improve performance. For instance, if the catalyst is optimized for direct functioning, the rate of backward reaction will be penalized, and the polarization curve for inverse operation will be slightly above the perfectly symmetric curve. So the curves are not symmetric anyway the two systems work exactly in the same manner, just inverted.

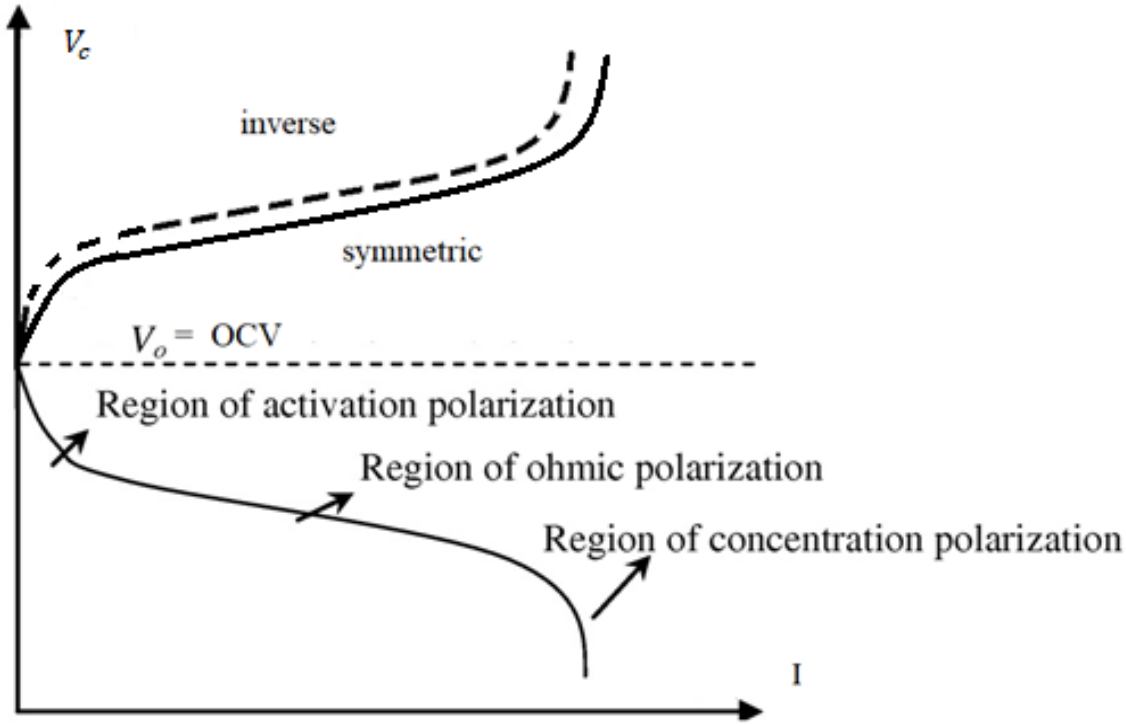

Fig. 2.3.1: Polarization Curve

Electrolyzers are applied to produce chemicals with high economic and thermodynamic values.

Commercial electrolyzers can be of three types:

- PEMEC (PEM electrolytic cell), where H^+ ions passing from anode to cathode
- SOEC (Solid Oxide Electrolytic cell), where O_2^- ions passing from cathode to anode
- AEC (Alkaline Electrolytic cell), where OH^- ions passing from the cathode to the anode

2.3.1 Electrolyzers comparison:

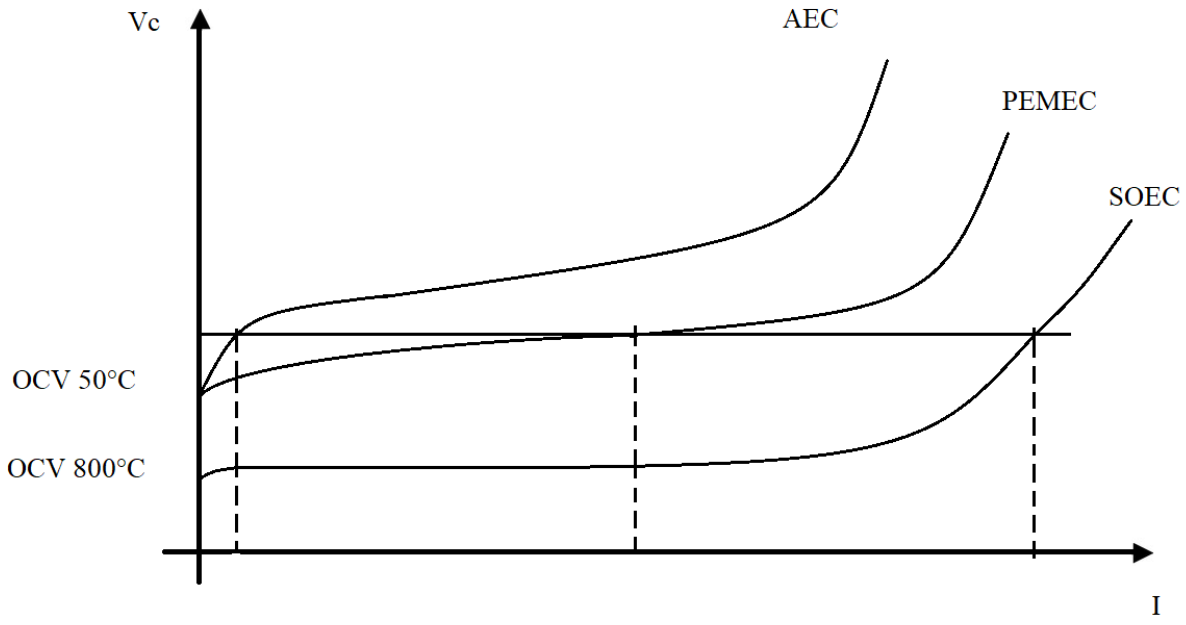

Fig.2.3.2: comparison between AEC, PEMEC, and SOEC

AEC always works in the exothermic regime, because the endothermic regime involves low voltage and currents and therefore low power produced. For this reason, a heat exchanger is always needed for an AEC to work, in order to remove heat produced by system operation.

SOEC is better performing because it is characterized by lower OCV, at a given current of operation, it requires a lower voltage.

Performances of an electrolyzer are measured with specific consumption E_{sp}: energy spent for Nm^3 of produced gas [kWh/Nm^3]. Actually, the specific consumption can be seen as the ratio between power adsorbed and volumetric flow rate of gas produced.

The lowest possible value of V_c is OCV. In the case of H_2O at a reference temperature of 25°C, OCV=1.23V.

The minimum specific consumption to split a water molecule is $E_{sp,\ min}$=2.44 x OCV=2.44 x 1.23=3.0012 kWh/Nm^3_{H2} =minimum theoretical energy required to produce 1m^3 of H_2 from water electrolysis.

In real operation E_{sp}=4.1/5.8 depending on the size optimized electrolyzer. In average E_{sp}=5 kWh/Nm^3_{H2}.

2.3.2 Fuel type

The type of gas produced will obviously affect by thermodynamic behavior of the system, thus different products will involve different polarization curve.

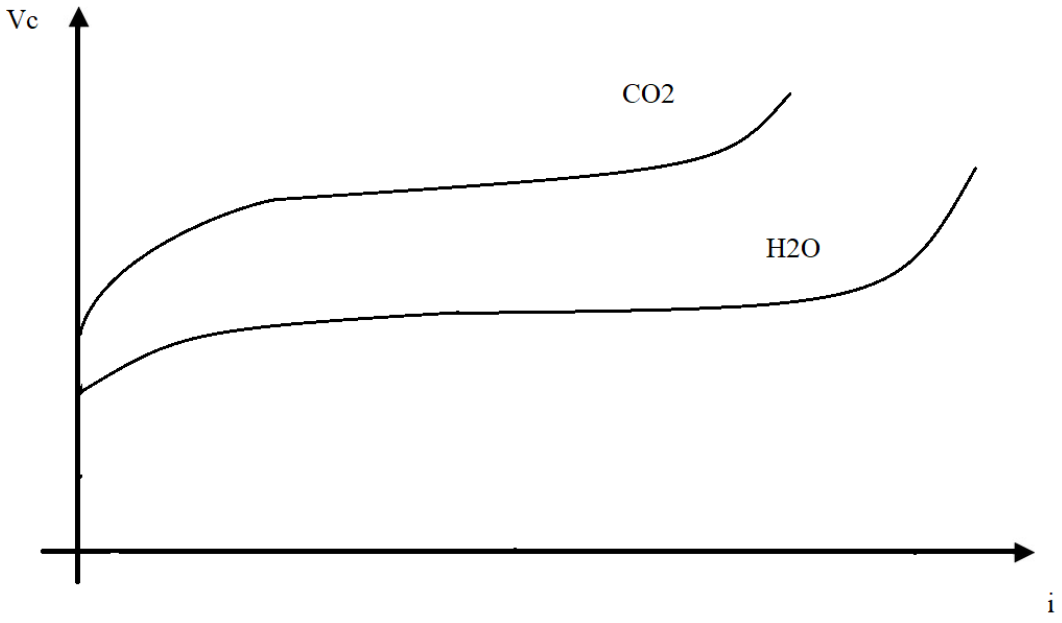

Fig. 2.3.3: Comparison between H_2O and CO_2

1st difference→ OCV is not the same, because we have two different reactions with different ΔG.

2nd difference→ kinetic of the two reactions are different.

However, the two curves have the same slope because the electrolyte layer is always the same.

2.3.3 AEC

Alkaline electrolyzer cells have been in commercial use in industrial applications since the 1920s and it is the most mature electrolyzer technology available today.

The electrolyte is an aqueous alkaline solution containing either sodium hydroxide (NaOH) or potassium hydroxide (KOH) and electrodes are commonly made of nickel coated steel.

AEC tend to use cheaper materials than PEMEC, due to their alkaline chemistry, which is also a consideration when raising the capital for a new installation.

In energy application, conventional AEC technology may have drawbacks, such as a relatively limited ability to respond to fluctuations in electrical input, something commonly found when integrating renewable such as wind and solar.

Gas purity is also the lowest, as traces of the electrolyte remain which must be scrubbed out in order to produce hydrogen of necessary purity.

These limitations are the subject of technology development aiming to improve the performance of AEC when linked to renewable energy, and new products targeting this application are being released.

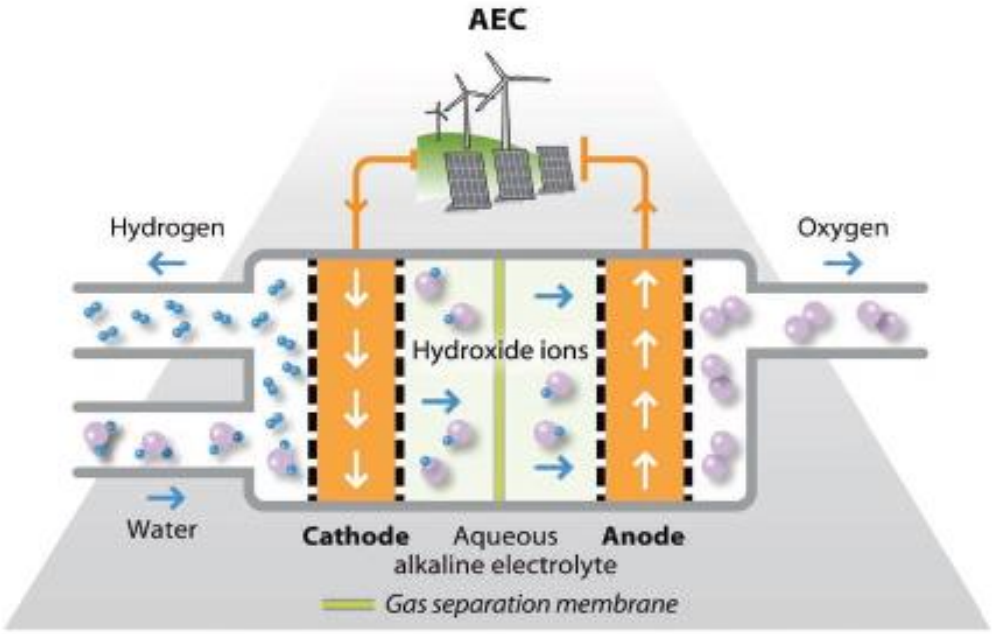

Fig. 2.3.4: AEC operation.

2.4 Electrolysis

When a voltage is imposed between two electrodes put into an electrolytic solution, an electric field is generated and it forces the migration of negative ions (anions) towards the anode and positive ions (cations) towards the cathode. At the same time, the oxidation at the anode with oxygen formation and the reduction at the cathode with hydrogen formation occur. In this way, the two elements are obtained as separated and a diaphragm avoids the mixing of them, allowing the passage of ions: this process is called electrolysis and the system is an electrolytic cell.

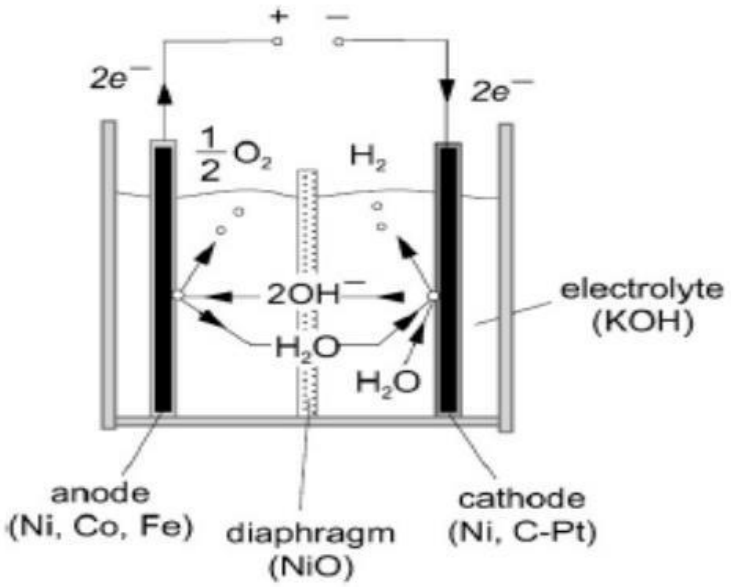

Fig. 2.4.1: typical structure of alkaline electrolyzer with KOH electrolyte.

The reactions occurring on an alkaline electrolyzer are the followings:

Cathode

$$4e^- + 4H_2O \rightarrow 2H_2 + 4OH^-$$

Anode

$$4OH^- \rightarrow O_2 + 2H_2O + 4e^-$$

Complete reaction

$$2H_2O \rightarrow 2H_2 + O_2$$

3 Self 25

The primary focus is the Electro Power System ‘ s plant, in particular to their Alkaline Electrolyzer, the objective of my study.

ENGIE EPS is the technological division of ENGIE which is focused on energy storage systems and microgrids, enabling the paradigm shift in the global energy system towards renewable sources and decentralized energy production.

ENGIE EPS’ mission is to accelerate the energy transition, turning renewable sources – by definition intermittent – into a stable power supply available on demand.

The technological heart of ENGIE EPS is HyESS (Hybrid Energy Storage System), a revolutionary proprietary technology that allows the integration of any renewable source, such as solar and wind, with all forms of energy storage, from lithium batteries to hydrogen.

Hydrogen Energy Storage System mainly consists of:

- Power-to-Gas module (Self25) composed by an AEC, that, thanks to the electrical power, can produce pressurized hydrogen and oxygen, which can be stored or reused as input in the PEMFC.

- Gas-to-Power module (Electro25) composed by a PEMFC, that is able to produce electrical power when is required using hydrogen and oxygen;

Furthermore, as well as P2G and G2P, the set-up consists of the following elements:

- The cooling system;
- the gas storage unit;
- the water refill plant;
- the master controller unit (is the electronic control system which sends the commands to the system through communication protocol ModBus TCP/IP);

- DC/DC converter;
- Local Controller Unit.

All of these modules are enclosed in a metal enclosure.

In order to build a model on the Power-to-Gas module, it is necessary a more detailed description of all its components.

3.1 General Concepts of Self 25

Self 25 is a fully integrated electrolyzer, the Power to Gas unit (P2G), equipped with an alkaline stack: it produces nominally 5 Nm^3/h of hydrogen (H_2) and 2,5 Nm^3/h of oxygen (O_2) using the water electrolysis reaction through the alkaline process. The core of the unit, the alkaline stack, converts electricity into storable chemical energy: H_2 and O_2 are indeed stored and exploited to generate electricity when required through *Electro 25*, the Gas to Power unit (G2P).

Self 25 and *Electro 25* are actually the two separated phases of an accumulator: *Self 25* represents the charge phase, while *Electro 25* represents the discharge phase.

Self 25, as *Electro 25*, are modular products, thought to be installed in series, in order to satisfy different accumulation and generation demands, just properly sizing the power output and the storage capability. They are indeed fundamental self-operating building blocks but managed at the plant level. With this logic, *Self 25* and *Electro 25* are the most adaptable integrators of big renewable parks, enable to modulate the irregular generation of renewable sources and to make them completely independent form diesel.

The P2G architecture unit includes, beyond the alkaline stack, the following parts, described in detail in the paragraph below:

1. separation unit;
2. electrolyte recirculation group;

3. venting group;
4. line to storage;
5. water refill circuit;
6. cooling circuit;
7. ventilation;

The table here below reports the main design data of *Self 25*.

Self 25		Unit	Design data
Features	Product		Self 25
	Type		Assembly
	Model		S 25
Size	Size	mm	1000x750x1100
	Weight	kg	750
Pressure	PS	barg	30
	Nominal operative pressure	barg	0 – 28,5
Temperature	TS	°C	+5 – +80
	Nominal operative temperature	°C	+5 – +80
Environment	Ambient temperature	°C	+5 – +35
	Relative humidity	%	30 - 85, without condensate
	Installation		Indoor
Fluids	Gas produced		H_2 and O_2
	Electrolyte		KOH 30%
Input	Nominal input power	kW	25
	Input voltage range	Vdc	450 – 550
	Input current range	A	0 – 60
	Water consumed	L	5
Output	H_2 produced	Nm^3/h	5
	O_2 produced	Nm^3/h	2,5
	Thermal power to dissipate	kW	8,5

Fig. 3.1.1: self 25 design data [10]

In the following figure, the main blocks topology of the system is reported; colors are used to highlight the different circuits: red for hydrogen, blue for oxygen, grey for cooling, ventilation and water refill, green for the electric circuit and purple for communication. The dotted box indicates the system cabinet boundaries; the dotted lines indicate the issues in charge of the User (safety and functional vents, storage lines, power input, cooling circuit).

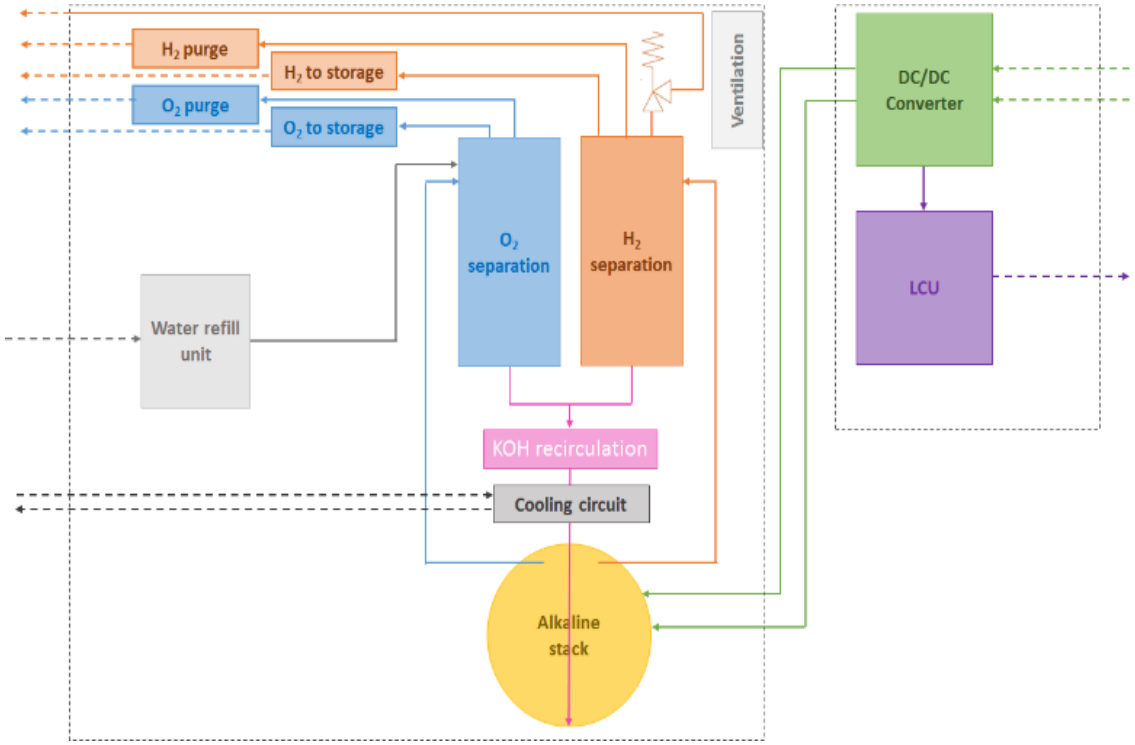

Fig. 3.1.2: Self 25 main block topology [10]

3.2 System Architecture

In this paragraph, the main blocks of the assembly shown in Figure 1 are described in details

3.2.1 Alkaline Stack

The alkaline stack is the electrochemical device in charge to convert electrical energy into chemical one, specifically into storable hydrogen and oxygen.

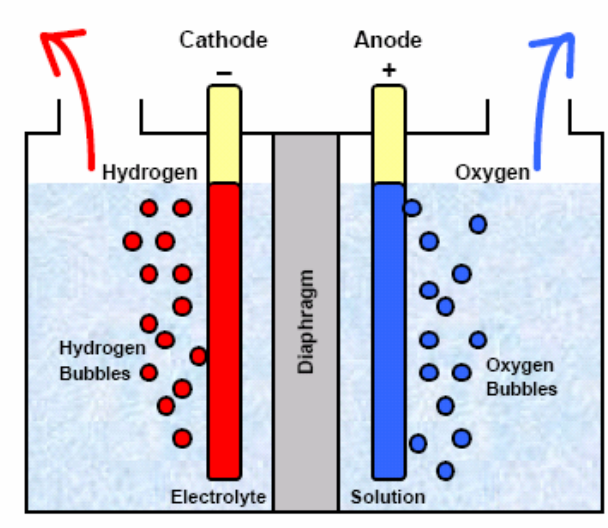

Fig. 3.2.1: Alkaline water electrolysis [10]

Water electrolysis occurs when a potential difference is applied between two electrodes immersed in an electrolytic solution (electrolyte and water); if the potential applied is higher than the water molecule dissociation potential, positive and negative ions are created and they move to the cathode (cations, negative electrode) and the anode (anions, positive electrode). In the meanwhile, ions near the electrodes react with the electrodes themselves.

Two half-reactions are involved:

At the cathode the reduction of water and the generation of hydrogen occur:

$$4e^- + 4H_2O \rightarrow 2H_2 + 4OH^-$$

At the anode the hydroxide ions are oxides to oxygen:

$$4OH^- \rightarrow O_2 + 2H_2\,O + 4e^-$$

The overall reaction is the following:

$$2H_2O \rightarrow 2H_2 + O_2$$

Hydrogen and oxygen are produced separately since the production occurs in the nearby of the electrodes and between the different poles, there is a membrane that avoids both gasses to get in contacts but let ions pass through.

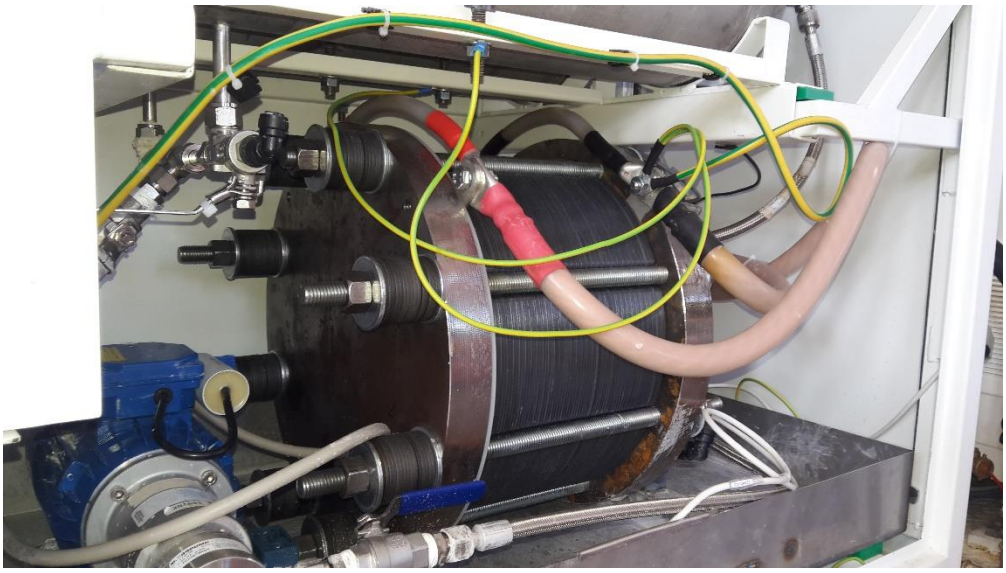

Fig. 3.2.2: E.EPS's alkaline stack

The alkaline stack is designed to absorb 25 kW in order to produce 5 Nm^3/h oh hydrogen and 2,5 Nm^3/h. The external devices composing the electrolyzer ensure the separation between the

produced gas and the electrolyte solution, the refill of the reactant (demineralized water) and the correct management of the system.

In the following figure, the list of the relevant design data of the alkaline stack is shown.

Parameter	Unit	Design Data
Number of cells		34
Active area	cm^2	452
Nominal power	kW	25
Hydrogen nominal production	Nm^3/h	5
Oxygen nominal production	Nm^3/h	2,5
Water consumption at nominal production	l/h	5
Concentration of KOH in electrolyte solution	%	30
Electrolyte flowrange	Nl/min	10
Stack PS	barg	0 / 33
Stack TS	°C	5 / 80
Stack current range	A	0 / 500
Stack voltage range	V	60 / 96
Stack Operative Temperature range	°C	5 / 80
Stack Ambient Temperature range	°C	+5 / +60

Fig. 3.2.3: alkaline stack design data [10]

3.2.2 Separation unit

Fig. 3.2.4: E.EPS separation tanks

Inside the separation tanks:

- hydrogen and oxygen get separated from the electrolyte solution;
- the electrolyte solution is degassed;
- the gas volumes are balanced by monitoring the electrolyte level.

Given that the water electrolysis reaction produces two hydrogen moles each oxygen mole, the volume occupied by the gases in the two separation tanks is always different. The monitoring of electrolyte level, made by two level sensors, each one consisting of four floating switches, is used to control the vent solenoid valves in order to balance the pressure inside the separation tanks. The four levels allow monitoring the situation inside the tanks with enough sensitivity.

The electrolyte volume prevents the mixing of the two produced gases and so the formation of an explosive atmosphere inside the tanks.

The separation tanks are designed for a p of 35 barg and they are properly protected by a pressure safety valve set at 30 barg.

3.2.3 Electrolyte recirculating group

The electrolyte recirculation group is made of:

- ✓ proper pipes,
- ✓ a pump,
- ✓ a heat exchanger,
- ✓ it is equipped with manual valves.

By using a forced recirculation of electrolytic solution, a better temperature distribution occurs.

The designed circuit ensures also the proper cooling of the electrolyte, checked by the thermoresistors installed on the circuit.

The manual valves allow on one hand the maintenance operation of refilling and, on the other, the drain of the electrolyte solution.

3.2.4 Venting group

The main purpose of the venting group is to balance the volume occupied by produced gases and electrolyte inside the separation tanks. The NO vent solenoid valves are indeed commanded by the level sensors. Upstream of the solenoid valves, different calibrated nozzles are placed in order to regulate the vent flow and avoid to unbalance the levels inside the tanks when one of the two valves open.

3.2.5 Line to storage

The gas pipes to storage are equipped with both NC solenoid valves and non-return valves.

The solenoid valves allow increasing the pressure of the system before storing the produced gas, while the non-return valves prevent from a reverse flow of gas from the storage to the system.

3.2.6 Water refill circuit

The demineralized water refill circuit implemented in the system allows a minimum level of autonomy to the system. It is still not enough to ensure lasting functionality; in fact, the user is in charge to add a properly sized water refill plant.

The water refill from the external plant is managed by the inlet solenoid valve, commanded by the level sensors of the water tank.

Demineralized water is conveyed to the oxygen separation tank: the reverse flow of oxygen is avoided thanks to the non-return valve installed.

3.2.7 Cooling circuit

The cooling circuit includes only the heat exchanger and a solenoid valve. The opening of this valve is controlled by the temperature of the electrolyte recirculation circuit.

The external cooling system must be properly sized and equipped with a recirculation pump able to ensure the necessary coolant flow.

3.2.8 Ventilation

The main purpose of the extraction fan, in combination with louver and monitoring flow sensor, is to guarantee the minimum dilution clean air flow rate by extraction and to remove heat from the containment enclosure.

The flow sensor delivers the status of the ventilation to the Local Controller. In case of failure, the system is lead to safety state both by alarm managed by the Local Controller and by the intervention of the safety module.

3.3 Operational state

Self 25 has 4 main operational states:

- ✓ Gas Production (On);
- ✓ Stand-by;
- ✓ Fault;
- ✓ Maintenance.

In order to pass from one operational state to another, there are some transient states and in particular:

- Initialization and Start;
- Normal cleaning and shutdown and Emergency cleaning and shutdown.

Please note that the monitoring is always on-line, in transient states as well.

Initialization_ The state “Init” occurs at the switch on and at this step the system is disabled and cannot receive any input. During the Init, the communication among the different electronic circuit boards (DC/DC, IO Alkaline stack) is verified and the proper configuration

files are uploaded. Just in case of positive results of the communication control, *Self 25* passes into “Stand-by” mode and is ready to be enabled from an external signal.

Start_ In this second transient state before the gas production (On mode), the forced ventilation of the cabinet starts and, if required, the separation tanks are refilled with demineralized water. At this point the system can start to produce gas.

On _ The state “On” indicates power generation. In this condition the electricity production is managed through the thermal, inlet, recirculation, vent and drain management.

Stand-by_ The “Stand-by” state is a passive state in which *Self 25* is not producing power. For safety purposes, some periodical controls are performed during this state.

Normal cleaning _ The “Normal cleaning” state must occur when the operation of the alkaline stack stops, without an emergency signal. When the unit stops to produce, leakage and pressure tests must be performed, then the system must be properly shut down and vented. The last item to be de-energized is the ventilation fan, only after having properly vented the internal volume of the cabinet.

Emergency cleaning_ In case of emergency shutdown, only an “emergency cleaning” is performed, during which the gases are safely vented outside the unit and any test is carried out. Also, in this state the ventilation keeps working until the safety renewed air supply is ensured.

Fault_ The “fault” state is a locked passive state in which *Self 25* is brought, passing through the cleaning state if necessary. In case of out of limits conditions (faults) the system shutdowns and goes into a locked state that requires an Operator intervention to be reset. In this way the system cannot turn on automatically until the cause of the fault has not been solved.

Maintenance_ In order to operate on the system in maintenance mode, the Operator has to set the key on the local controller unit in the maintenance position. Using a proper human interface connected to the local controller unit and entering the username and password, the “Maintenance” state is enabled and the Operator can operate on the system.

3.4 Hydrogen

Hydrogen is/has:

- a colorless and odorless gas,
- easily inflammable,
- extremely reactive, especially with oxygen
- subject to igniting spontaneously if it flows out at high speeds,
- lighter than air,
- asphyxiating at high concentrations,
- a flammable range (in air) of 4 – 75 %,
- an explosive range (in air) of 15 – 59% and
- ignition temperature of 500 °C.

Given the wide explosive and flammable range of hydrogen in air, even small leaks of hydrogen have the potential to burn or explode. Leaked hydrogen tends to accumulate on the top of an enclosed environment, being lighter than air, and can concentrate on it, increasing the risk of combustion and explosion.

Hydrogen flames are pale blue and are almost invisible in daylight due to the absence of soot. Due to its high buoyancy and diffusivity, burning hydrogen rises unlike gasoline, which spreads laterally.

A flammable or explosive hydrogen mixture is easily ignited by a spark or even a hot surface. The energy of a hydrogen gas explosion is 2.4 times that of gasoline or methane for an equal volume. Hydrogen gas explosions are therefore more destructive and carry further.

An adequate air change rate must be ensured and/or an extraction system and an approved hydrogen sensor must be installed.

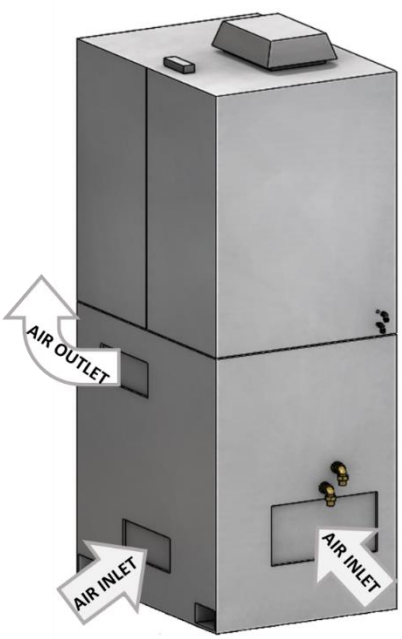

Fig. 3.4.1: Air openings on the cabinet of Self 25

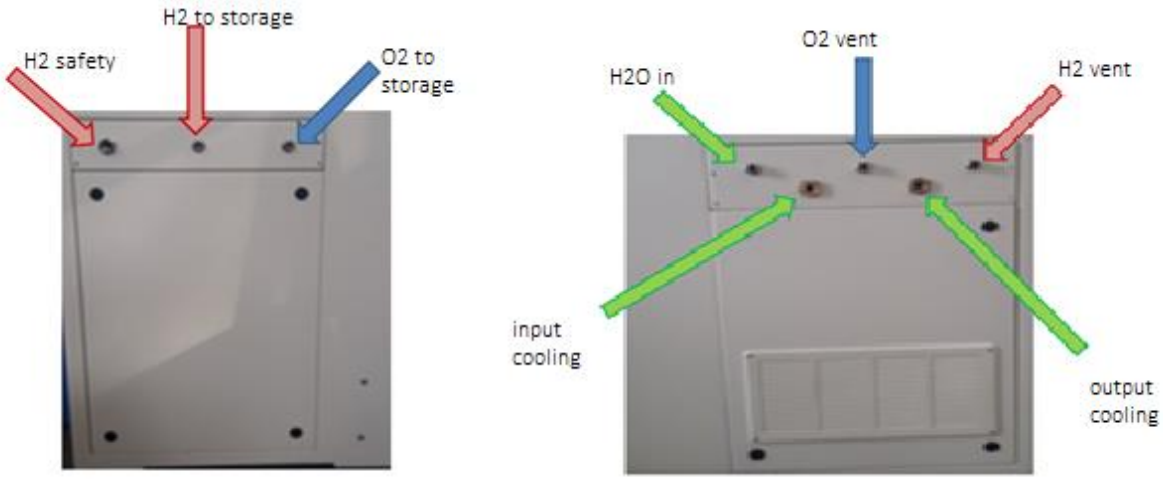

Fig. 3.4.2: Vent pipe of hydrogen and oxygen

Prevent overexposure to hydrogen. Hydrogen is non-toxic but can act as a simple asphyxiating by displacing the oxygen in the air. There are no warnings before unconsciousness results. When operating the stack in an enclosure:

- Ensure ventilation slots are clear and unobstructed at all times during operation.
- Operate within the temperature's limits stated in the manual.
- Never operate if an alarm condition exists.

Constant exposure to hydrogen causes hydrogen embrittlement in many materials. Factors known to influence the rate and severity of hydrogen embrittlement include hydrogen concentration, hydrogen pressure, temperature, hydrogen purity, type of impurity, stress level, stress rate, metal composition, metal tensile strength, grain size, microstructure and heat treatment history. Moisture content in the hydrogen gas may lead to metal embrittlement through the acceleration of the formation of fatigue cracks. Hydrogen embrittlement can lead to leakage or catastrophic failures in metal and non-metallic components.

3.5 Oxygen

Oxygen is/has:

- A colorless, odorless and tasteless gas;
- A non-toxic gas;
- Essential for life in appropriate concentrations;
- is a highly reactive nonmetal;
- is an oxidizing agent that readily forms oxides with most elements as well as other compounds.

Highly concentrated sources of oxygen promote rapid combustion. Fire and explosion hazards exist when concentrated oxidants and fuels are brought into close proximity; an ignition

event, such as heat or a spark, is needed to trigger combustion. Oxygen is the oxidant, not the fuel, but nevertheless the source of most of the chemical energy released in combustion.

The result of breathing increased partial pressures of oxygen is hyperoxia, an excess of oxygen in body tissues. The body is affected in different ways depending on the type of exposure. Central nervous system toxicity is caused by short exposure to high partial pressures of oxygen at greater than atmospheric pressure. Pulmonary and ocular toxicity result from longer exposure to increased oxygen levels at normal pressure. Symptoms may include disorientation, breathing problems, and vision changes such as myopia. Prolonged exposure to above-normal oxygen partial pressures, or shorter exposures to very high partial pressures, can cause oxidative damage to cell membranes, a collapse of the alveoli in the lungs, retinal detachment, and seizures. Oxygen toxicity is managed by reducing the exposure to increased oxygen levels. Studies show that, in the long term, robust recovery from most types of oxygen toxicity is possible.

3.6 Potassium hydroxide

Potassium hydroxide is:

- a white, solid, hygroscopic compound
- extremely soluble in water
- highly corrosive

Flakes of potassium hydroxide as well as aqueous solution of this compound are very hazardous in case of skin contact (corrosive, irritant), of eye contact (irritant, corrosive), of ingestion, of inhalation. The amount of tissue damage depends on the length of contact. Eye contact can result in corneal damage or blindness. Skin contact can produce inflammation and blistering. Inhalation of dust will produce irritation to gastro-intestinal or respiratory tract, characterized by burning, sneezing and coughing. Severe over-exposure can produce lung damage, choking unconsciousness or death. Inflammation of the eye is characterized by

redness, watering, and itching. Skin inflammation is characterized by itching, scaling, reddening, or, occasionally, blistering.

Potassium hydroxide is a corrosive chemical that is normally handled in either steel, nickel, nickel alloys or certain types of plastic equipment. The most common construction materials for handling and storing potassium hydroxide solutions are black iron and mild steel.

However, liquid potassium hydroxide will attack these metals at elevated temperatures.

Aluminum, copper, zinc, lead, tin and their alloys (e.g., brass and bronze) are NOT suitable. Potassium hydroxide readily attacks these materials. In addition, considerable heat is generated when liquid or dry potassium hydroxide is mixed with water, which can result in boiling or splattering and may cause a violent eruption. When diluting, always add potassium hydroxide to water. Never add water to potassium hydroxide.

In order to avoid the unwanted release of caustic fluid under pressure, the electrolyte circuit manual valves are equipped with the locked closed device, which the User must proper manage.

4 Theoretical model

In this chapter, it is described the mathematical model used to obtain the outlet gas impurity of the alkaline electrolyzer.

The knowledge of the lower operating range is mandatory when the alkaline electrolyzer is dynamically operated with a renewable energy source. Thus, this study provides a zero-dimensional model based on a classical process engineering approach for the prediction of the resulting hydrogen and oxygen purity.

Furthermore, a description of the experimental determination of necessary parameters and the model validation via online gas purity measurements is presented.

The presented model is taken from [11].

4.1 A mathematical model of the alkaline electrolyzer

The aim of the developed model is to estimate the resulting gas purity of an alkaline water electrolyzer as a function of the current density, electrolyte flow rate and temperature.

In alkaline electrolysis, the electrodes are immersed in a 20-40% potassium hydroxide solution and separated by a diaphragm or membrane to keep the evolved product gases apart. [12]

During electrolysis, hydrogen is formed at the cathode, whereas oxygen production takes place at the anode.

At the cathode the reduction of water and the generation of hydrogen occur:

$$2e^- + 2H_2O \rightarrow H_2 + 2OH^-$$

At the anode the hydroxide ions are oxidized to oxygen:

$$2OH^- \rightarrow ½O_2 + H_2O + 2e^-$$

The overall reaction is the following:

$$H_2O \rightarrow H_2 + ½O_2$$

Caused by the different consumption and production of water in the half cells, an electrolyte concentration gradient is formed. Therefore, the anodic and cathodic electrolyte cycles are continuously mixed to compensate for this difference in electrolyte concentration.

However, this cycling strategy limits the typical operating range to 10-40% of the nominal load as the oxygen purity is drastically reduced through the contamination of hydrogen below this limit. The sources of this contamination are the diffusion through the separator and the mixing of the gas-saturated electrolyte solution, which enables dissolved species to reach the opposite gas separator. [13]

The electrolyte cycling strategy considered is the ‘mixed mode’, where anolyte and catholyte are mixed continuously to compensate for the difference in electrolyte concentration caused by the half cell reactions.

The overall model concept is based on classical gas-liquid-reactors with physical absorption as shown in figure 4.1.1.

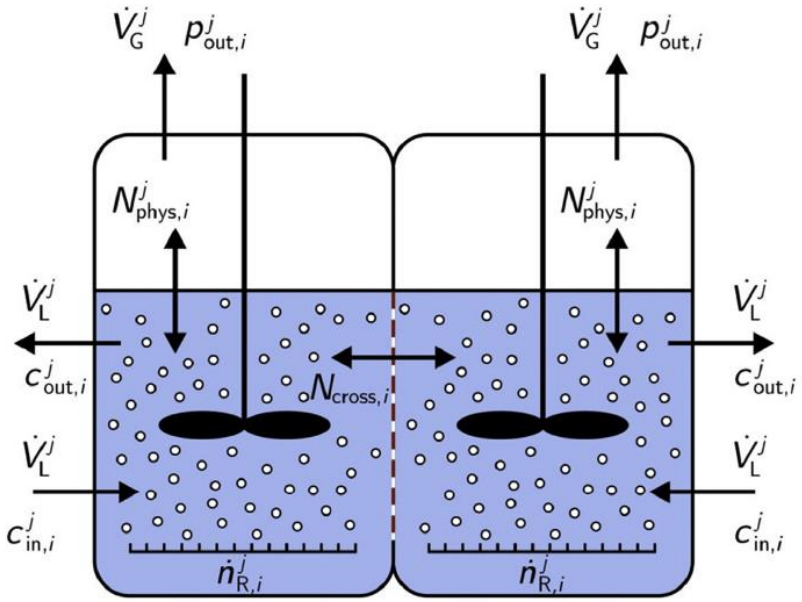

Fig. 4.1.1: Basic CSTR model concept of the electrolysis cell with occurring fluxes. Compartment j = anodic, cathodic; species i= H_2, O_2, H_2O [11].

The electrolysis cell is divided into two continuous stirred-tank reactors (CSTR), which are connected through a separator allowing a crossover $N_{cross,\ i}$ of dissolved species i, being hydrogen and oxygen.

Each half cell is fed with a gas-free flow of the electrolyte solution $\dot{V}_L^j$, whereas gas is evolved at the electrodes with the molar flow rate $\dot{n}_{R,i}^j$ caused by the electrochemical reactions.

To estimate the gas partial pressures $p_{out,i}^j$ and liquid concentrations $c_{out,i}^j$ at the anodic and cathodic exit of the electrolysis cell, it is necessary to implement a heterogeneous two-phase model which considers the phase mass transfer $N_{phys,i}^j$ through physical absorption and desorption of the species. In practice, the two-phase flow, represented by $\dot{V}_L^j$ and $\dot{V}_G^j$, leaves the electrolysis cell and enters a gas-liquid-separator, which depicts the model flowsheet derived from the lab-scale electrolyzer.

Within this model, it is assumed that no further phase transition takes place within the separators as the effective mass transfer area and the coefficient is small compared to the

electrolysis cell. This is caused by bubble coalescence within the tubing behind the exit of the cell and an approximately stagnant fluid in the separators. It is further assumed that the separators behave perfectly so that only dissolved gases are recycled to the electrolysis cell whereas gas bubbles are removed completely. In ‘mixed mode’ both electrolyte cycles from the anodic and cathodic chamber are merged before they are fed to the electrolysis cell again. In figure 4.1.2, this electrolyte pathway is indicated in green, whereas the ‘separated mode’ (where both cycles are separated from each other to prevent the contamination of the opposite product gas through gas dissolution) is shown in dashed purple. We will consider only the ‘mixed mode’.

Furthermore, other assumptions and simplifications are made which are summarized in the following:

- stationary process
- ideal CSTR behavior with constant temperature and concentration
- water saturated product gasses
- film model for the mass transfer
- neglect of the recombination reaction and assumption of 100% faradaic efficiency
- monodisperse bubble size distribution
- no mass transfer in pipes and gas separators
- ideal mixer

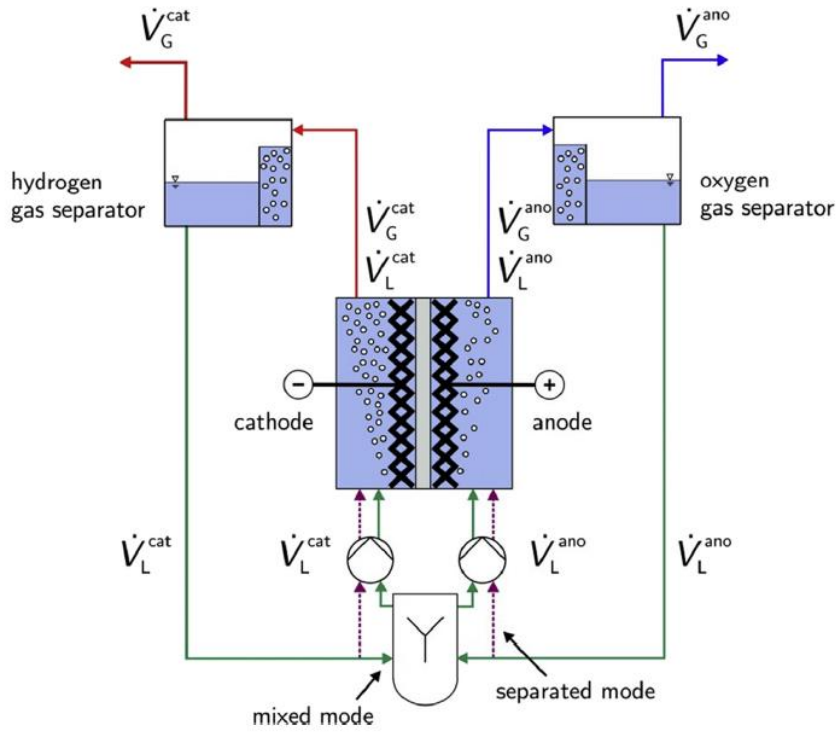

Fig.4.1.2: Model flowsheet derived from lab-scale electrolyzer [11]

The considered gaseous species are hydrogen, oxygen and water whilst only hydrogen and oxygen are taken into account for the liquid phase balance. The crossover through the separator is assumed to occur only in the liquid phase as the solid phase of the separator is reported to be impermeable for gases. [14].

Any variations of the OH^- concentrations are assumed to be negligible because of the highly concentrated electrolyte and the continuous replacement of the consumed water in the experimental setup.

In the following chapters, the model equations and boundary conditions are explained in detail. [11]

4.1.1 Material balance

The material balance of the electrolysis half cells relies on a classical two-phase CSTR, which is a common ideal reactor in chemical engineering [15]. This reactor type is chosen as the half cells are well mixed [16] through gas evolution, which is the reason for bubble induced electrolyte convection [17], and turbulence due to electrolyte entering the cell through nozzles.

The liquid electrolyte enters the half cells with dissolved amounts of hydrogen and oxygen. In the electrolysis cell, hydrogen and oxygen are electrochemically produced on the electrodes according to the electrochemical equations. It is assumed that hydrogen and oxygen are produced in the dissolved form [18] before gas bubbles grow at active nucleation sites on the electrodes or in the electrolyte bulk.

Thus the electrolysis products leave the electrode boundary layer either in dissolved or in gaseous form. This effect is considered in the material balances for the gas and liquid phase through the gas evolution efficiency $f_{G,i}$, which describes the fraction of product leaving the electrode boundary layer in the gaseous phase [19]. A more detailed description of these phenomena is given in the following chapter "Electrochemical reaction". The mass transfer between the electrolyte bulk and the gaseous phase is considered using a desorption or absorption flux $N_{phys,i}^{j}$, whereas the crossover through the separator is described through $N_{cross,i}$, which needs to be added to the liquid anodic material balance and subtracted from its cathodic counterpart. This is due to the definition of the concentration gradient in Fick's law, which is explained in the chapter "Crossover through the separator" in detail.

With these assumptions the stationary anodic and cathodic liquid and gaseous material balances write as follows:

Anode liquid:

$$\dot{V}_L^{ano} \cdot \left(c_{in,\mathrm{i}}^{ano} - c_{out,\mathrm{i}}^{ano}\right) + N_{phys,\mathrm{i}}^{ano} \cdot A_{GL}^{ano} + N_{cross,\mathrm{i}} \cdot A_{sep} + \left(1 - f_{G,i}\right) \cdot \dot{n}_{R,\mathrm{i}}^{ano} = 0 \qquad (1)$$

Cathode liquid:

$$\dot{V}_L^{cat} \cdot \left(c_{in,i}^{cat} - c_{out,i}^{cat}\right) + N_{phys,i}^{cat} \cdot A_{GL}^{cat} - N_{cross,i} \cdot A_{sep} + \left(1 - f_{G,i}\right) \cdot \dot{n}_{R,i}^{cat} = 0 \quad (2)$$

Gas:

$$\frac{\dot{V}_G^j}{R \cdot T} \cdot \left(p_{in,i}^j - p_{out,i}^j\right) - N_{phys,i}^j \cdot A_{GL}^j + f_{G,i} \cdot \dot{n}_{R,i}^j = 0 \quad (3)$$

Where:

- i are the species: H_2 and O_2
- j are the compartment: anode and cathode

The solution of these material balances necessitates boundary conditions, which can be derived from the previously described assumptions, electrolyte management strategies and the flowsheet of the electrolyzer model. [11]

In case of mixing anolyte and catholyte both half cells are fed with the same liquid concentration of dissolved species c_i^{mix} from the ideal mixer. Thus the following boundary condition applies:

$$c_{in,i}^j = c_i^{mix} \quad (4)$$

As it is assumed that no gas bubbles are recycled from the separators back to the electrolysis cell the inlet partial pressures of the species can be set to zero.

$$p_{in,i}^j = 0 \quad (5)$$

The absolute pressure of the evolving gas bubbles is defined by an equation which is the sum of the applied pressure p^0 to the system and an additional pressure Δp^j, which results from

the concave curvature of the spherically shaped gas bubbles. This additional pressure can be estimated by applying the Younge-Laplace equation [20].

$$p^j = p^0 + \Delta p^j \tag{6}$$

$$\Delta p^j = \frac{4 \cdot \gamma}{d_b^j} \tag{7}$$

Here γ denotes the surface tension of the electrolyte, which is calculated according to the data provided by Feldkamp [21].

$$\gamma = \sum_{n=0}^{3} \gamma_n \cdot (w_{KOH})^n \tag{8}$$

γ_0	0.06588789
γ_1	0.02454658
γ_2	0.1283735
γ_3	-0.0330648

As the product gases can be assumed to be saturated with water the water partial pressure p_{H_2O} is equal to the water vapor pressure of the KOH solution, which can be calculated according to Balej [22] in dependence on the electrolyte temperature and concentration. Thus the following relationship between the absolute pressure and the partial pressures of the species applies:

$$p^j = \sum p_{out,i}^j + p_{H_2O} \tag{9}$$

$$log(p_{H_2O}) = -0.01508 \cdot m_{KOH} - 0.0016788 \cdot (m_{KOH})^2 + 2.25887 \cdot 10^{-5} \cdot (m_{KOH})^3 + (1 - 0.0012062 \cdot m_{KOH} + 5.6024 \cdot 10^{-4} \cdot (m_{KOH})^2 - 7.8228 \cdot 10^{-6} \cdot (m_{KOH})^3) \cdot (35.4462 - \frac{3343.93}{T} - 10.9 \log(T) + 0.0041645 \cdot T) \quad (10)$$

$$m_{KOH} = \frac{w_{KOH}}{M_{KOH}(1 - w_{KOH})} \quad (11)$$

Finally, the exit mole fraction of the species can be accessed with the following equation, which considers the removal of water from the exhaust gas flows.

$$x_{out,i}^{j} = \frac{p_{out,i}^{j}}{p^{j} - p_{H_2O}} \quad (12)$$

For completion of the model, the material balance of the mixing unit is required. With the assumption of an ideal mixer, the material balance can be written as follows:

$$\dot{V}_L^{mix} \cdot c_i^{mix} = \sum \dot{V}_L^{j} \cdot c_{out,i}^{j} \quad (13)$$

4.1.2 Electrochemical reaction

The molar flow rates of the species generated at the electrodes can be calculated with the applied current density J, the electrode area A_{el} and the Faraday Constant F according to Faraday's law.

The stoichiometric coefficients of the products can be derived from equations and amount to $\nu_{H_2}^{cat} = 1$ and $\nu_{O_2}^{ano} = 0.5$ if the number of electrons transferred z is set to two.

$$\dot{n}_{R,i}^{j} = \frac{J \cdot A_{el} \cdot \nu_i^j}{F \cdot z} \quad (14)$$

As already mentioned, the electrolysis products are generated in dissolved form before the growth of gas bubbles becomes possible within the electrode boundary layer. The dissolved species produced there are either transported to the gas-liquid interface of adhering bubbles or to the electrolyte bulk. Since the gas solubility in the highly concentrated alkaline media is low, the electrode boundary layer becomes strongly oversaturated. This supersaturation is mandatory for bubble growth at the electrode as a sufficient deviation from equilibrium is necessary for a nucleation site to become active [23]. Nucleation sites are small electrode surface irregularities, which are strongly dependent on the kind of material or its roughness [24].

As soon as a nucleation site becomes active bubbles are formed through the supply of dissolved species from the surrounding supersaturated electrolyte. Whether gas is evolved at the electrode or dissolved species are transported to the bulk depends on the operating conditions of the electrolyzer. At low current densities, nearly the total amount of produced species is transported to the bulk as the concentration gradient at the electrode is too low for the activation of nucleation sites [25].

If the current density is increased bubbles start to grow at the electrode surface as the supersaturation of the electrolyte becomes high enough to enable diffusion into the gaseous

phase. This behavior can be described through the introduction of the gas evolution efficiency $f_{G,i}$, which denotes the fraction of product generated as gas bubbles within the electrode boundary layer [19]. The remaining fraction leaves the boundary layer in dissolved form and may be transported into rising bubbles in a subsequent mass transfer step.

Next to the current density, the gas evolution efficiency is also affected by the electrode material, electrode potential and the amount of produced gas [25]. It should be noted that the gas evolution efficiency only reaches unity at very high current densities, while it is significantly smaller in typical electrolysis processes [23].

In the present study, the gas evolution efficiency is considered a fitting parameter, because of no data for the hydrogen and oxygen evolution reaction under technical relevant conditions, namely 30 wt% KOH and 65 °C, could be found. A description of the fitting procedure is given in the chapter "Gas evolution efficiency".

4.1.3 Mass transfer

The fraction of electrolysis products, which reaches the electrolyte bulk in dissolved form, can be incorporated into the surrounding rising bubbles [23]. This effect is considered by the application of the film theory and the introduction of a species-specific mass transfer coefficient $k_{L,i}^{j}$.

$$N_{phys,i}^{j} = k_{L,i}^{j} \cdot (c_i^{*j} - c_{out,i}^{j}) \quad (15)$$

As the electrolyte is supersaturated with the electrolysis products this mass transfer mainly occurs into the direction of the gaseous phase. In film theory, the assumption of a stagnant film between the interconnected phases is made, in which mass transfer only occurs by diffusion. At this interface, the gaseous and liquid concentration is assumed to be in

equilibrium [26]. If the mass transfer resistance is further assumed to be controlled by the liquid film the liquid equilibrium concentration c_i^{*j} can be estimated with Henry's law.

This assumption is permissible as the solubility of the gases is low [27]. For the estimation of the Henry coefficients in the pure water, the correlation by Himmelblau [28] was applied, which is necessary for the calculation of the gas solubility in highly concentrated alkaline media using the Setchenov relation [29]. Therefore the Setchenov constants of the species need to be known, which are achieved by fitting the data provided by Knaster and Apel'baum [30].

Hydrogen and oxygen solubility in aqueous potassium hydroxide solution:

$$\log\left(\frac{c_{i,H_2O}^*}{c_i^{*j}}\right) = k_i \cdot w_{KOH} \tag{16}$$

k_{H_2}	3.14
k_{O_2}	3.66

$$c_{i,H_2O}^* = \frac{\rho_{H_2O}}{M} \cdot \frac{p_{out,i}^j}{101325 \cdot H_i} \tag{17}$$

$$\rho_{H_2O} = \left(\sum_{n=0}^{5} \rho_{H_2O,n} \cdot (\vartheta)^n\right) \Big/ (1 + 16.879850 \cdot 10^{-3} \cdot \vartheta) \tag{18}$$

$\rho_{H_2O,0}$	999.83952
$\rho_{H_2O,1}$	16.945176
$\rho_{H_2O,2}$	$-7.9870401 \cdot 10^{-3}$
$\rho_{H_2O,3}$	$-46.170461 \cdot 10^{-6}$
$\rho_{H_2O,4}$	$105.56302 \cdot 10^{-9}$
$\rho_{H_2O,5}$	$-280.54253 \cdot 10^{-12}$

Henry coefficients of hydrogen and oxygen in water:

$$A(log\overline{H_i})^2 + B(1/\bar{T})^2 + C(log\overline{H_i})(1/\bar{T}) + D(log\overline{H_i}) + E(1/\bar{T}) - 1 = 0 \qquad (19)$$

With: $\overline{H_i} = H_i/atm \cdot 10^{-4}$ and $1/\bar{T} = (1/T/K) \cdot 10^3$ and

Gas	A	B	C	D	E
H_2	-0.1233	-0.1366	0.02155	-0.2368	0.8249
O_2	-0.0005943	-0.1470	-0.05120	-0.1076	0.8447

This equation has two solutions: the best solution is the biggest.

For the estimation of the mass transport coefficient in gas-liquid reactors, a variety of Sherwood-Reynolds correlations can be found in the literature. The Reynolds number Re results from the physical properties of the electrolyte, the gas bubble diameter d_b^j and the bubble swarm velocity u_{sw}^j [31].

$$Re = \frac{\rho_L \cdot d_b^j \cdot u_{sw}^j}{\eta_L} \quad (20)$$

Where:

$$\rho_L = \left(\sum_{n=0}^{4} \rho_{L,n} \cdot (\vartheta)^n \right) \cdot \exp(0.86 \cdot w_{KOH}) \quad (21)$$

$\rho_{L,0}$	1001.53053
$\rho_{L,1}$	-0.08343
$\rho_{L,2}$	-0.00401
$\rho_{L,3}$	$5.51232 \cdot 10^{-6}$
$\rho_{L,4}$	$-8.20994 \cdot 10^{-10}$

And

$$\eta_L = \left(\sum_{n=0}^{4} \eta_{L,n} \cdot (T)^n \right) \quad (22)$$

$\eta_{L,0}$	0.9105535967
$\eta_{L,1}$	-0.01062211683
$\eta_{L,2}$	$4.680761561 \cdot 10^{-5}$
$\eta_{L,3}$	$-9.209312883 \cdot 10^{-8}$
$\eta_{L,4}$	$6.814919843 \cdot 10^{-11}$

ϑ is the temperature value expressed in °C.

The estimation of the bubble swarm velocity necessitates the rise velocity of a single gas bubble, which can be calculated with the equation by Peebles and Garber [32] for spherical gas bubbles with inner circulation at Re >2 [33]. However, the literature provides diverse information about the validity of this equation. According to Kienzlen [34], this equation is also applicable for the estimation of the hydrogen bubble rise velocity in 30 wt% KOH in the range from 1 < Re < 430. Thus, this equation is applied for the cathodic as well as the anodic bubble rise velocity.

$$u_b^j = 0.33 \cdot g^{0.76} \cdot \left(\frac{\rho_L}{\eta_L}\right)^{0.52} \left(\frac{d_b^j}{2}\right)^{1.28} \quad (23)$$

A gas bubble, which rises within a swarm, experiences a reduction of the effective rise velocity due to collisions of these bubbles. Kreysa and Kuhn [35] summarized a variety of bubble swarm velocity correlations as a function of the single bubble rise velocity u_b^j and the gas voidage ε_g^j. Here, the reduction of the rise velocity is considered with the equation proposed by Brauer and Thiele [36].

$$u_{sw}^j = u_b^j \cdot \frac{1}{1 + \frac{\varepsilon_g^j}{\left(1 - \varepsilon_g^j\right)^2}} \cdot \frac{1 - \varepsilon_g^j}{1 + \frac{1.05}{\left(1 + \frac{0.0685}{\left(\varepsilon_g^j\right)^2}\right)^{0.5}} - 0.5} \quad (24)$$

Under operating conditions of our electrolyzer, the mentioned equations lead to Reynolds numbers in the magnitude of Re ~ 1. Additionally, the Schmidt number Sc_i is mandatory for the estimation of the Sherwood number Sh_i^j and the mass transfer coefficient, respectively. It is defined by the physical properties of the liquid and the gaseous diffusion coefficient $D_{i,k}$ in the electrolyte.

$$Sc_i = \frac{\eta_L}{\rho_L \cdot D_{i,k}} \tag{25}$$

With these equations, it is now possible to find an appropriate Sherwood correlation. We used the equation developed by Brauer and Mewes [31] which is valid for spherical bubbles and Re -> 0.

$$Sh_i^j = \frac{k_{L,i}^j \cdot d_b^j}{D_{i,k}} = 2 + \frac{0.651 \cdot \left(Re^j \cdot Sc_i\right)^{1.72}}{1 + \left(Re^j \cdot Sc_i\right)^{1.72}} \tag{26}$$

Thus, mass transfer coefficients for hydrogen and oxygen in the magnitude of $k_{L,i}^j$ ~10^4 m/s are achieved. A comparison with equation by Wesselingh and Krishna [26] for small particles or bubbles yields similar values.

$$k_{L,i}^j = \frac{2 \cdot D_{i,k}}{d_b^j} \tag{27}$$

It was shown in the material balance equations that the interfacial area A_{GL}^j is required for the calculation of the phase transition fluxes. For an estimation of this area, the gas holdup ε_g^j in the electrolysis half cells must be known. Therefore, the gas fraction $\varepsilon_{g,out}^j$ at the outlet of the

electrolysis cell was experimentally determined, which is described in the chapter “Gas holdup”. However, this measuring method leads to higher gas hold up values than in the electrolysis cell as the gas bubbles coalesce in the tubing behind the cell exit, which causes the pressure of the gaseous phase to decrease since the overpressure due to the spherical shape disappears. Thus, the gas volume and hold up in the electrolysis half cells can be assessed with the following equations.

$$V_{gas}^{j} = \varepsilon_{g,out}^{j} \cdot V_{hcell} \cdot \frac{p^{0}}{p^{j}} \quad (28)$$

$$\varepsilon_{g,out}^{j} = \frac{V_{gas}^{j}}{V_{hcell}} \quad (29)$$

For reasons of simplification, a monodisperse bubble size distribution is assumed. For a given gas bubble diameter d_b^j, the volume V_b^j and surface area S_b^j of a single spherical bubble can then be achieved through geometrical relationships.

$$V_b^j = \frac{\pi}{6} \cdot \left(d_b^j\right)^3 \quad (30)$$

$$S_b^j = \pi \cdot \left(d_b^j\right)^2 \quad (31)$$

Finally, the overall interfacial area between the liquid and gaseous phase A_{GL}^{j} writes as follows:

$$A_{GL}^{j} = \frac{V_{gas}^{j}}{V_{b}^{j}} \cdot S_{b}^{j} \tag{32}$$

4.1.4 Crossover through the separator

The separator in an alkaline water electrolysis cell has the functions to prevent short circuits between the electrodes and to avoid the mixing of evolved hydrogen and oxygen. For this purpose, the separator needs to be stable under highly alkaline conditions and very conducive for the transport of OH^- ions. The conductivity of a separator mainly depends on its porosity and tortuosity as the current passes through the liquid electrolyte in the pores [37]. Furthermore, these properties influence the transport of dissolved gas through the separator. In PEM (proton exchange or polymer electrolyte membrane) electrolysis modeling gas crossover is typically described through a combination of differential pressure driven convection and diffusional species transport across the membrane. For a proper estimation of these crossover fluxes the electrolyte supersaturation with electrolysis products, which was mentioned in chapter “Electrochemical reaction”, should be considered as it may enhance the overall species transport across the separator [38]. Alkaline water electrolyzers, however, are usually operated with equal anodic and cathodic pressures, so that only diffusional crossover occurs, which can be described by application of Fick’s law.

$$N_{cross,i} = \frac{D_{i,k}^{eff}}{d_{sep}} \cdot \left(c_{out,i}^{cat} - c_{out,i}^{ano}\right) \tag{33}$$

In this equation, d_{sep} denotes the separator thickness, whereas $c_{out,i}^{j}$ is the cathodic and anodic concentration of dissolved gas and $D_{i,k}^{eff}$ the effective diffusion coefficient of the species in the separator. According to the equation a positive diffusion flux is achieved if the cathodic is greater than the anodic outlet concentration. This is the case for hydrogen as its liquid concentration is generally higher in the cathodic compartment. This results in a flux of dissolved hydrogen from the cathodic to the anodic half cell. Therefore, this flux needs to be subtracted from the liquid, cathodic material balance and added to its anodic counterpart. Moreover, in the case of oxygen, the equation delivers a negative flux, as the oxygen concentration is always greater in the anodic compartment. This is valid for the anodic material balance, as oxygen diffuses from the anodic to the cathodic compartment. However, in the cathodic compartment, this flux needs to be subtracted for an addition to the material balance equation. This is the reason why $N_{cross,i}$ is provided with a positive sign in the anodic and a negative sign in the cathodic compartment [11].

The calculation of the effective diffusion coefficient requires the molecular diffusion coefficient $D_{i,k}$ in the electrolyte because the pores are filled with the liquid solution. These binary diffusion coefficients are calculated from polynomials, which represent the data provided by Tham et al. [39] and are shown. Furthermore, the porosity and tortuosity of the separator are required for the estimation of the effective diffusion coefficient.

$$D_{i,k}^{eff} = D_{i,k} \cdot \frac{\varepsilon}{\tau} \tag{34}$$

Where the binary diffusion coefficients of hydrogen and oxygen in aqueous potassium hydroxide solution are:

$$D_{H_2,KOH} = \sum_{n=0}^{2} D_{H_2,KOH_n} \cdot (w_{KOH})^n \quad (35)$$

$$D_{O_2,KOH} = \sum_{n=0}^{3} D_{O_2,KOH_n} \cdot (w_{KOH})^n \quad (36)$$

	H_2 – 60°C	O_2 – 60°C
$D_{i,KOH,0}$	$8.04542 \cdot 10^{-9}$	$4.27612 \cdot 10^{-9}$
$D_{i,KOH,1}$	$-2.07309 \cdot 10^{-8}$	$-1.90911 \cdot 10^{-8}$
$D_{i,KOH,2}$	$2.02214 \cdot 10^{-8}$	$3.6684 \cdot 10^{-8}$
$D_{i,KOH,3}$	-	$-2.53386 \cdot 10^{-8}$

In alkaline water electrolysis, the aforementioned electrode boundary layer is strongly oversaturated with the dissolved electrolysis product. The succeeding mass transfer pathway of the product is usually controlled by two competing mechanisms.

Thus, the product is either transported to the electrolyte bulk in dissolved form or to the liquid-gas interface of bubbles present in the electrode boundary layer, which is considered through the gas evolution efficiency. This implies, that the flux of dissolved gas from the electrode to the electrolyte bulk changes with electrode distance [40]. Furthermore, the dissolved product may also be transported through the separator. As the electrodes are directly pressed into the diaphragm in a zero-gap configuration, the supersaturated concentration within the electrode boundary should actually be applied for estimation of the diffusional crossover flux.

However, due to the assumption of an ideal CSTR with uniform concentration distribution the local concentration gradient from the electrode to the electrolyte bulk cannot be considered in this model yet. Therefore, the model predicts a lower crossover flux through the separator than experimentally determined, as a smaller concentration gradient across the separator is applied for calculation.

4.2 Experimental determination of modeling parameters

The experimental parametrization and validation of the model presented in this study was performed and described in detail in the published paper [41] and [11].

Furthermore, the model application needs the determination of unknown operational parameters, such as the gas evolution efficiency, gas bubble diameter, and gas volume in the electrolysis half cells.

A description of the determination and applied measurement techniques are also given in the following.

4.2.1 Gas evolution efficiency

It was mentioned in the chapter "Electrochemical reaction" that the gas evolution efficiency is considered a fitting parameter as no information about the hydrogen and oxygen evolution efficiency at technical relevant conditions is available in the literature.

The equation used for f_{G,H_2} is taken from [11].

$$f_{G,H_2} = 0.25744 \cdot J^{0.14134} \quad (37)$$

Thusly achieved values are in good agreement with the data reported by Chin Kwie Joe et al. [42], which may be attributed to the similar operating conditions.

However, the anodic gas evolution efficiency could hardly be determined by application of the method mentioned above.

The cathodic oxygen impurity is typically small compared to the anodic hydrogen content due to the higher production rate of hydrogen, which is evolved in a molar ratio of 2:1 compared to oxygen.

This problem is assumed to be caused by an underestimation of the anodic oxygen mass transfer from the liquid to the gaseous phase, which leads to an overestimated dissolved oxygen concentration entering the cathodic half cell. Furthermore, it is possible that the neglected reduction of dissolved oxygen to water at the cathode is responsible for the lower cathodic oxygen content.

In this model the oxygen gas evolution efficiency is defined as:

$$f_{G,O_2} = (0.25744 \cdot J^{0.14134}) - 0.01 \quad (38)$$

Although this is physically incorrect, a scientific analysis should be carried out in order to optimize this equation.

4.2.2 Gas bubble diameter

The gas bubble diameter has an impact on the gas purity in alkaline water electrolysis as it directly influences the mass transfer area of the liquid and gaseous interface. Usually, gas bubbles detach from the electrode surface as soon as buoyancy and shear forces exceed the adhesion forces [23]. However, it is difficult to solve this equilibrium of forces as many parameters, such as the roughness of the electrode, the contact angle and the electrolyte velocity in the vicinity of the electrode surface have to be known. Therefore, simplified empirical relations have been developed, which relate the breakoff diameter to operational characteristics of the electrolyzer.

Vogt and Balzer [43] found that the diameter $d_{b,0}^{j}$ estimated with the modified Fritz equation, which is usually applied in heat transfer calculations and valid at zero current, shows good agreement with the regression lines of their measuring data.

$$\frac{d_b^j(J)}{d_{b,0}^j} = (1 + 0.2 \cdot J)^{-0.45} \quad (39)$$

There is still disagreement in the literature about the exact bubble diameter dependence as it is strongly influenced by the electrode material, the electrolyte, and possible additives. Therefore, the bubble diameter in our electrolysis cell was experimentally determined as no specific data for the used electrodes and electrolyte solution could be found in the literature. During the experiments, the current density and electrolyte flow rate were systematically varied in order to achieve surface area data as a function of these parameters.

In this model the equations used are:

$$d_b^{cat} = 593.84 \cdot (1 + 0.2 \cdot J)^{-0.25} \quad (40)$$

$$d_b^{ano} = (593.84 \cdot (1 + 0.2 \cdot J)^{-0.25}) - 4 \cdot 10^{-5} \quad (41)$$

Although these equations are physically incorrect, a scientific analysis should be carried out in order to optimize the equations.

4.2.3 Gas holdup

It was shown in chapter "Mass transfer" that the gas holdup is necessary for the calculation of the bubble swarm velocity and the interfacial area between the liquid and gaseous phase. Due to the application of a highly concentrated potassium hydroxide solution in the electrolysis process, it is possible to perform conductivity measurements for the determination of the gas voidage at the outlet of the electrolysis cell. The electrical conductivity of a liquid is reduced through the dispersion of gas within this solution and directly related to the gas voidage through the Bruggemann equation [44].

$$\frac{k_L}{k_{L,0}} = \left(1 - \varepsilon_{g,out}^{j}\right)^{3/2} \quad (42)$$

Here $k_{L,0}$ and k_L denote the conductivity of the gas-free liquid and the dispersion, respectively. For the determination of the gas voidage $\varepsilon_{g,out}^{j}$ the outgoing gas-liquid flows of the cathodic and anodic compartment were led through a measurement cell.

These studies have built for different values of current density and flow rate.

In this model the data are given from the paper [11], though these values are physically incorrect, a scientific analysis should be carried out in order to verify the validity of these values.

Compartment	X1	X2	X3
Anodic	0.59438	0.59231	0.75647
Cathodic	0.76764	0.73233	0.73457

$$\varepsilon_{g,out}^{j} = X1 - X2 \cdot X3^{(J/1000)} \quad (43)$$

4.3 Data used in the model

The data used in the model are taken from E.EPS, the litterature and the model considered:

Parameter	Value	Source
N_{cell}	34 [-]	E.EPS
A_{el}	$452 \cdot 10^{-4}$ [m^2]	E.EPS
$\dot{V}_L^{KOH}$	10 [L/min]	E.EPS
$\dot{V}_L^{cat}$	5 [L/min]	E.EPS
$\dot{V}_L^{ano}$	5 [L/min]	E.EPS
r_c	120 [mm]	E.EPS
d_c	5.5 [mm]	E.EPS
r_{sep}	125 [mm]	E.EPS
d_{sep}	0.5 [mm]	E.EPS
w_{KOH}	30 %	E.EPS
V	70 [V]	E.EPS
T	65 [°C]	E.EPS
p^0	15 [bar]	E.EPS
P_{in}	22.5 [kW]	E.EPS
M_{KOH}	0.0561056 [kg/mol]	Literature
R	8.314 [J/(mol·K)]	Literature
F	96.485 [C/mol]	Literature
G	9.823 [m/s^2]	Literature
M_{H_2O}	0.018 [kg/mol]	Literature
E	0.5 [-]	Literature
T	3.14 [-]	Literature
k_{H_2}	3.14 [m/s]	Literature
k_{O_2}	3.66 [m/s]	Literature

Starting from the data, a Matlab model has built, in order to calculate the other parameters described above. Different scripts have built in order to solve the system equations.

After the calculation of the other values the system of non-linear equation is solved, using 'fsolve' function on Matlab.

In particular, the system is composed of 12 equations. Equations (1), (2), and (3) became:

$$\dot{V}_L^{ano} \cdot \left(c_{H2}^{mix} - c_{out,H2}^{ano}\right) + N_{phys,H2}^{ano} \cdot A_{GL}^{ano} + N_{cross,H2} \cdot A_{sep} + \left(1 - f_{G,H2}\right) \cdot \dot{n}_{R,H2}^{ano} = 0 \quad (44)$$

$$\dot{V}_L^{ano} \cdot \left(c_{O2}^{mix} - c_{out,O2}^{ano}\right) + N_{phys,O2}^{ano} \cdot A_{GL}^{ano} + N_{cross,O2} \cdot A_{sep} + \left(1 - f_{G,O2}\right) \cdot \dot{n}_{R,O2}^{ano} = 0 \quad (45)$$

$$\dot{V}_L^{cat} \cdot \left(c_{H2}^{mix} - c_{out,H2}^{cat}\right) + N_{phys,H2}^{cat} \cdot A_{GL}^{cat} - N_{cross,H2} \cdot A_{sep} + \left(1 - f_{G,H2}\right) \cdot \dot{n}_{R,H2}^{cat} = 0 \quad (46)$$

$$\dot{V}_L^{cat} \cdot \left(c_{O2}^{mix} - c_{out,O2}^{cat}\right) + N_{phys,O2}^{cat} \cdot A_{GL}^{cat} - N_{cross,O2} \cdot A_{sep} + \left(1 - f_{G,O2}\right) \cdot \dot{n}_{R,O2}^{cat} = 0 \quad (47)$$

$$\frac{\dot{V}_G^{ano}}{R \cdot T} \cdot \left(p_{in,H_2}^{ano} - p_{out,H_2}^{ano}\right) - N_{phys,H_2}^{ano} \cdot A_{GL}^{ano} + f_{G,H_2} \cdot \dot{n}_{R,H_2}^{ano} = 0 \quad (48)$$

$$\frac{\dot{V}_G^{ano}}{R \cdot T} \cdot \left(p_{in,O_2}^{ano} - p_{out,O_2}^{ano}\right) - N_{phys,O_2}^{ano} \cdot A_{GL}^{ano} + f_{G,O_2} \cdot \dot{n}_{R,O_2}^{ano} = 0 \quad (49)$$

$$\frac{\dot{V}_G^{cat}}{R \cdot T} \cdot \left(p_{in,H_2}^{cat} - p_{out,H_2}^{cat}\right) - N_{phys,H_2}^{cat} \cdot A_{GL}^{cat} + f_{G,H_2} \cdot \dot{n}_{R,H_2}^{cat} = 0 \quad (50)$$

$$\frac{\dot{V}_G^{cat}}{R \cdot T} \cdot \left(p_{in,O_2}^{cat} - p_{out,O_2}^{cat}\right) - N_{phys,O_2}^{cat} \cdot A_{GL}^{cat} + f_{G,O_2} \cdot \dot{n}_{R,O_2}^{cat} = 0 \quad (51)$$

The BC's equations (9) and (13) became:

$$\dot{V}_L^{ano} \cdot c_{out,O2}^{ano} + \dot{V}_L^{cat} \cdot c_{out,O2}^{cat} = \dot{V}_L^{mix} \cdot c_{O2}^{mix} \quad (52)$$

$$\dot{V}_L^{ano} \cdot c_{out,H2}^{ano} + \dot{V}_L^{cat} \cdot c_{out,H2}^{cat} = \dot{V}_L^{mix} \cdot c_{H2}^{mix} \quad (53)$$

$$p^{cat} = p_{out,O_2}^{cat} + p_{out,H_2}^{cat} + p_{H_2O} \quad (54)$$

$$p^{ano} = p_{out,O_2}^{ano} + p_{out,H_2}^{ano} + p_{H_2O} \quad (55)$$

The 12 variables to calculate are:

- p_{out,O_2}^{ano}
- p_{out,H_2}^{ano}
- p_{out,O_2}^{cat}
- p_{out,H_2}^{cat}
- c_{out,O_2}^{ano}
- c_{out,H_2}^{ano}
- c_{out,O_2}^{cat}
- c_{out,H_2}^{cat}
- $c_{O_2}^{mix}$
- $c_{H_2}^{mix}$
- $\dot{V}_G^{ano}$
- $\dot{V}_G^{cat}$

After solving the system and using the other formula descrived above to calculate the outlet mole fraction, the outlet gas purity is founded.

4.4 Validation and results of gas purity modeling

The first graph of the model is obtained considering the current density variation.

As you can see, the value of hydrogen in oxygen at the anode side and the value of oxygen in hydrogen at the cathode side decreases with increasing current density: in fact, for low value of current density the gas impurity is too much high, while for high value of current density the gas impurity reach convergence.

From this first result, it can be understood that is better for the electrolyzer to work at high power in order to have a better value of gas purity.

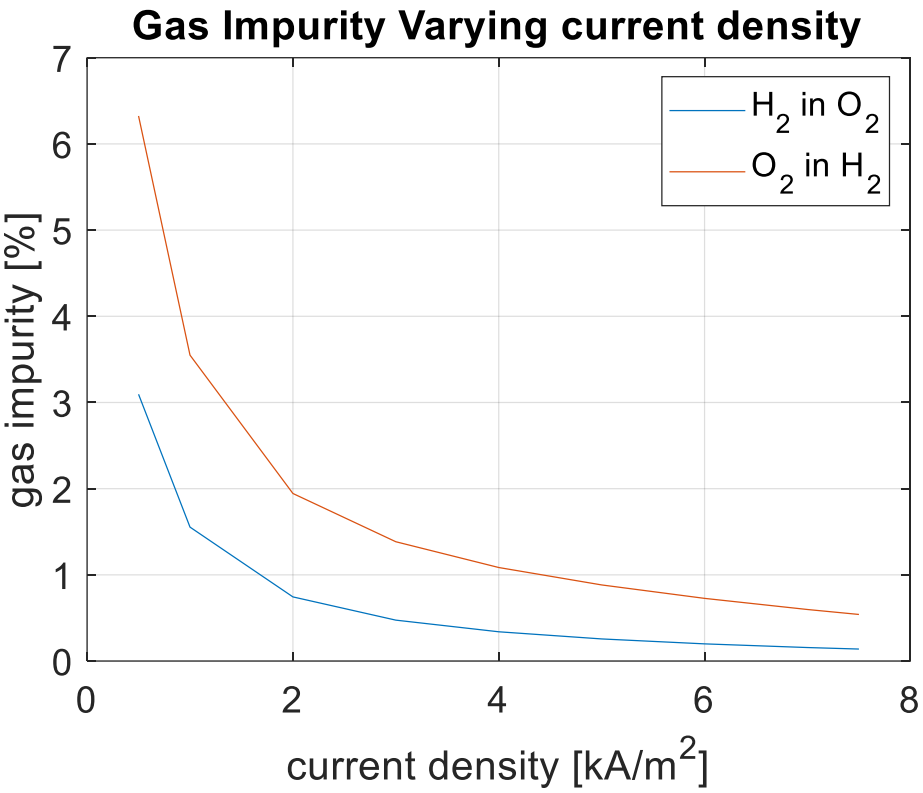

Fig. 4.4.1: Gas purity varying the current density at the anode (blue line) and at the cathode (red line)

The following sensitivity analyses have been performed:

- Varying the volumetric liquid electrolyte flow rate of KOH respectively at the anode and cathode side.

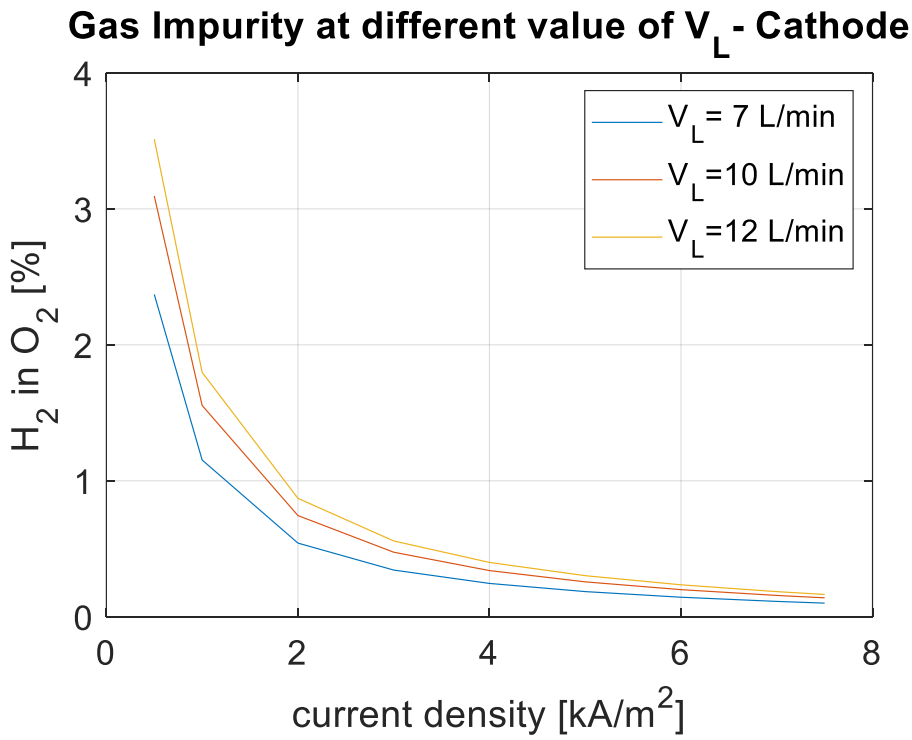

Fig. 4.4.2: Gas purity varying the electrolyte flow rate- Cathode

Three different electrolyte flow rates were fed for investigating the impact of electrolyte flow rate in gas purity.

As you can see in both cases with the growing of electrolyte flow rate the gas purity decreases.

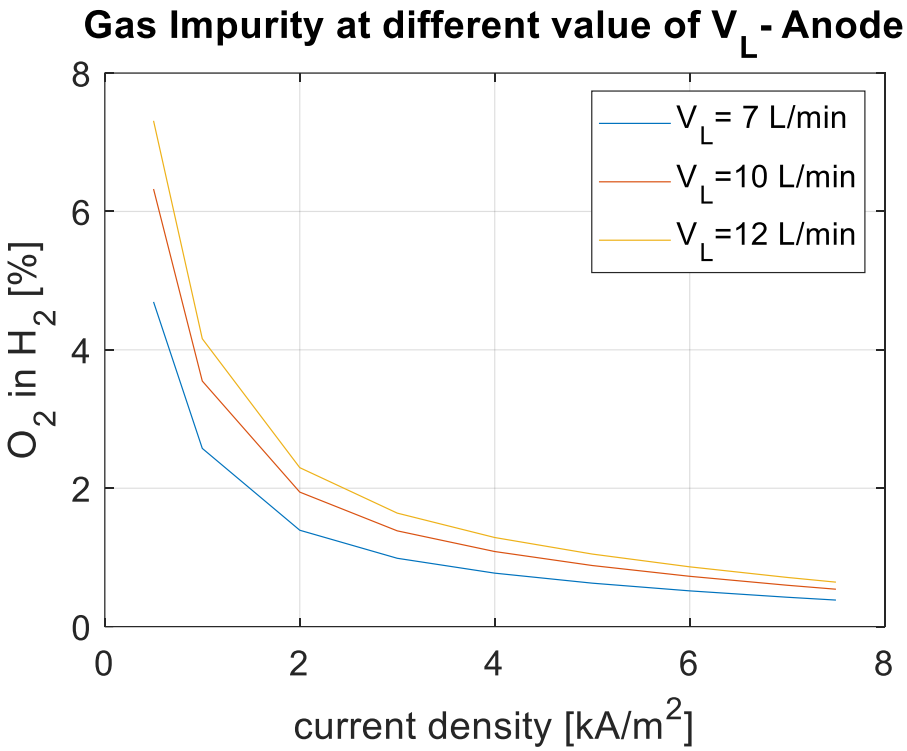

Fig. 4.4.3: Gas purity varying the electrolyte flow rate- Anode

- Varying the mass fraction of KOH in electrolyte solution respectively at the anode and cathode side. The electrolyte concentration directly influences both gas solubility and diffusion coefficients of the dissolved species. The gas solubility mostly decreases with a growing electrolyte concentration.

The figures 4.4.4 and 4.4.5 showing how electrolyte concentration affect gas purity.
In fact, with the growth of the KOH mass fraction the gas purity increases.
This is a relevant result that can be useful in order to optimize the system's works.

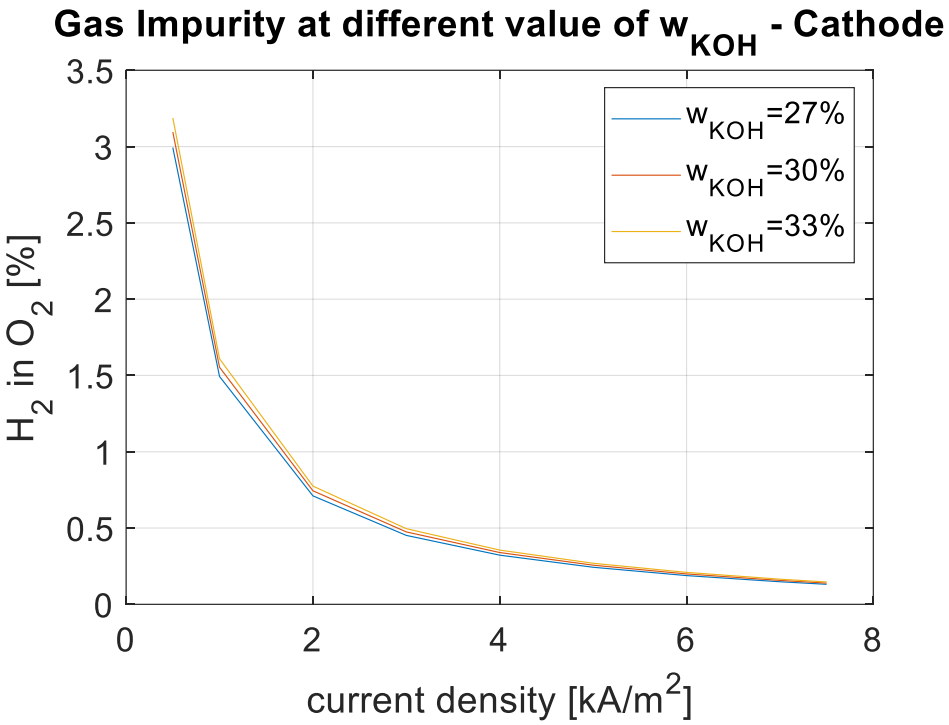

Fig. 4.4.4: Gas purity varying the KOH concentration - Cathode

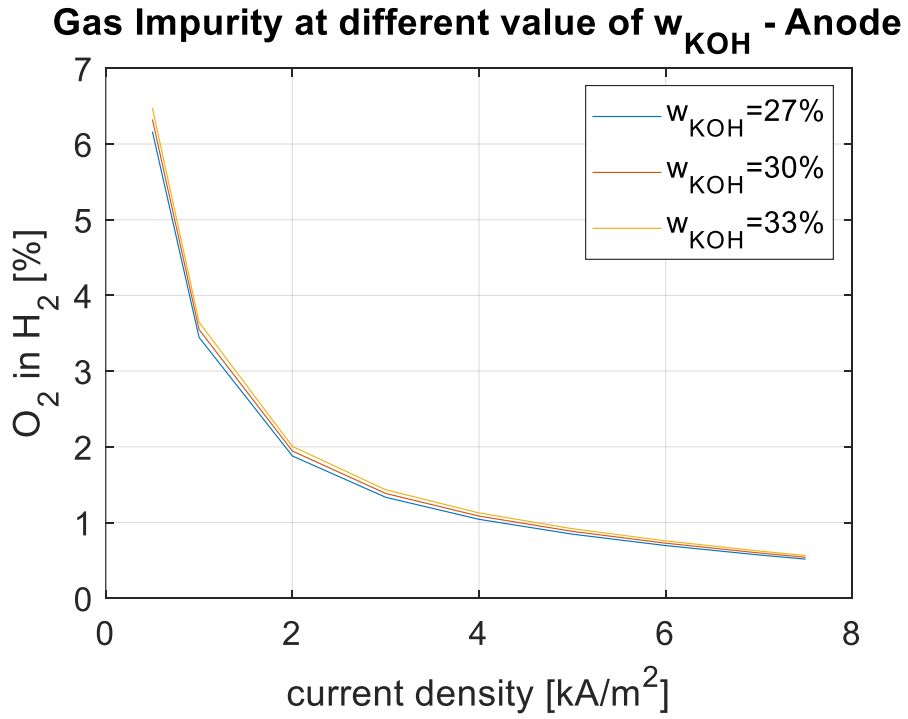

Fig. 4.4.5: Gas purity varying the KOH concentration - Anode

5 Test and Results

The previous chapter explains the model used in order to know the percentage of hydrogen in oxygen at the anode side and the percentage of oxygen in hydrogen at the cathode side.

This model was build in order to understand the values that influenced the gas purity at the exit of the Alkaline electrolyzer, but in this model, some parameters are fitting parameters and many hypothesis has to be done.

This chapter presents the experimental results obtained by the company's tests.

Moreover, this chapter presents the model validation through a comparison of the modeling results and the experimentally determined product gas purity.

5.1 Operation test

At first, is able to understand which are the operational data of Self 25.

Self 25 works at a nominal power of 22 kW, the temperature range is 60-70°C, and the voltage range is 60-70 V.

Self 25 has a purity sensor at the exit of the cathode side that estimates the percentage of oxygen in hydrogen.

The hope is to minimize this percentage in order to have pure hydrogen at the exit of the electrolyzer.

Results obtained from the model, as mentioned previously, have many hypotheses: in particular, the applied system pressure p^0 was a constant value, instead, the applied system pressure of Self 25 increases during his works, starting from 0 bar and at the end is 16 bar fixed.

The results shown below are dependent on the varying pressure.

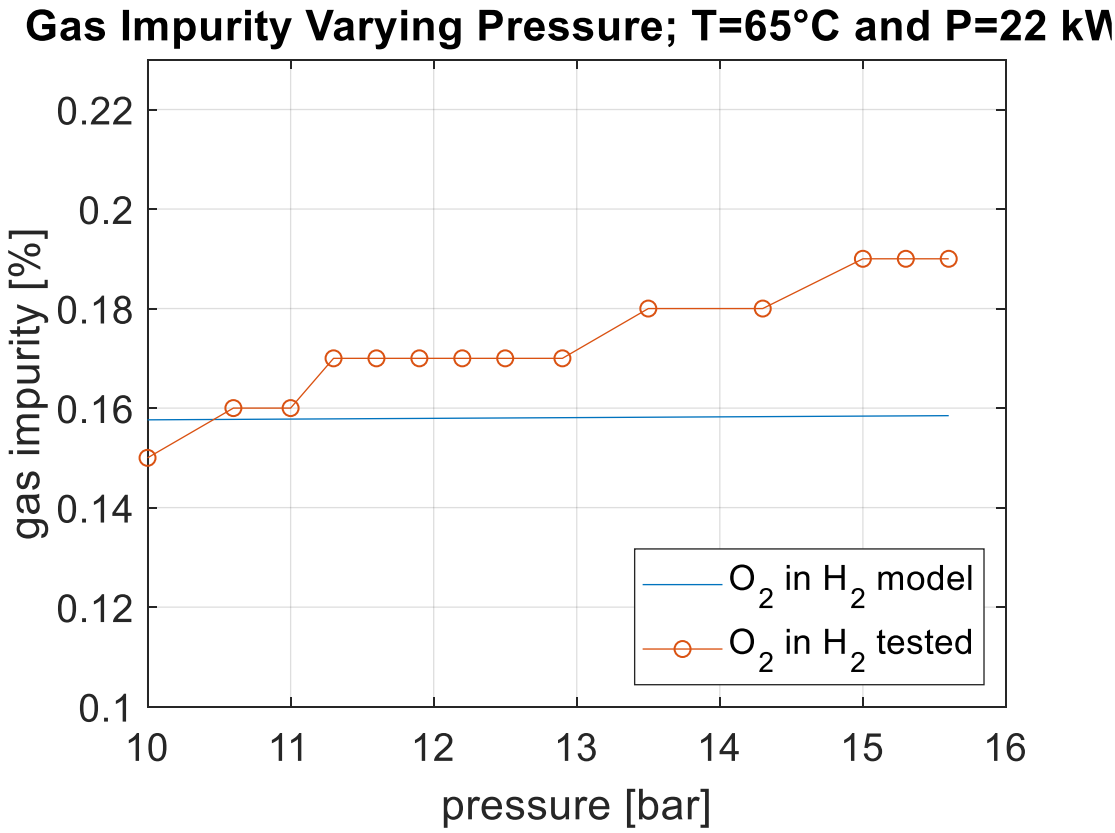

Fig. 5.1.1: Gas purity at operating conditions

As you can see the percentage of oxygen in hydrogen obtained from the model consists of an almost straight line: the values increase with pressure but slightly.

The results obtained from the company's test are values taken point by point with increasing pressure.

The increase in the values obtained from the tests is greater than that obtained from the model.

5.2 Experimental tests

Let's consider now the change of such parameters. After the results obtained from the model and the comparison with the operating test, other different experimental tests were made.

Considering that in Self 25 was impossible to change values such as the KOH concentration % and the electrolyte flow rate, the other two important parameters has been changed.

5.2.1 Case 1 – Temperature variation

At first, is important to know how the outlet gas purity change at different value of temperature. So two company's tests were made and the results are shown below.

Case 1 – Test 1

For the first test, the value of temperature from 65°C to 60°C has been changed.

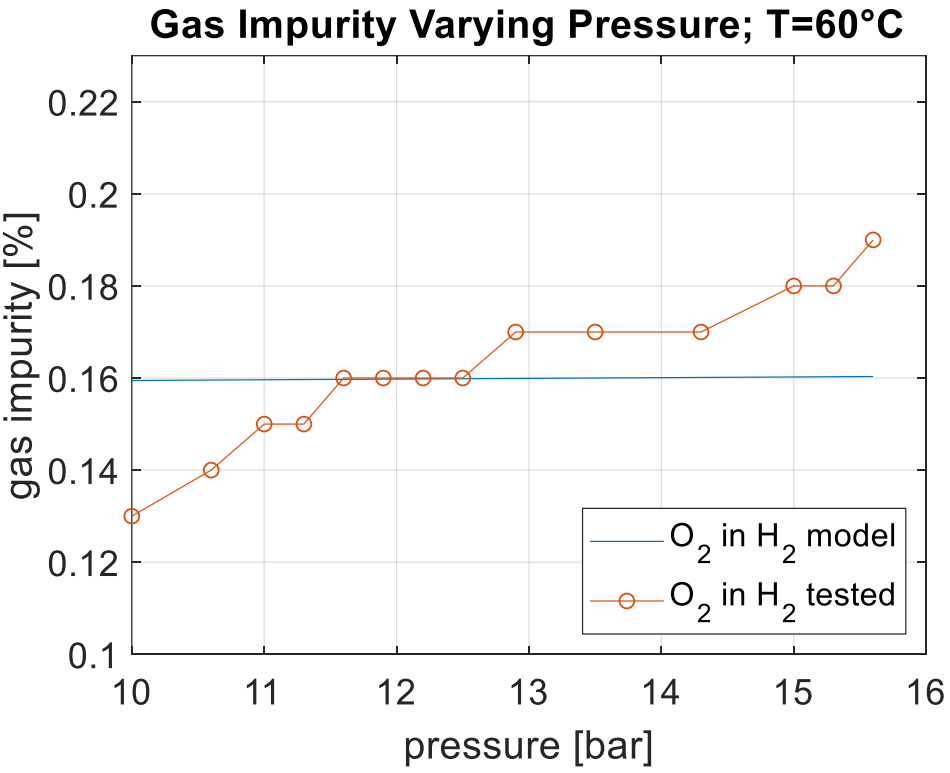

Fig. 5.2.1: Gas purity at T=60 °C

Case 1 – Test 2

For the second test, the value of temperature from 65°C to 55°C has been changed.

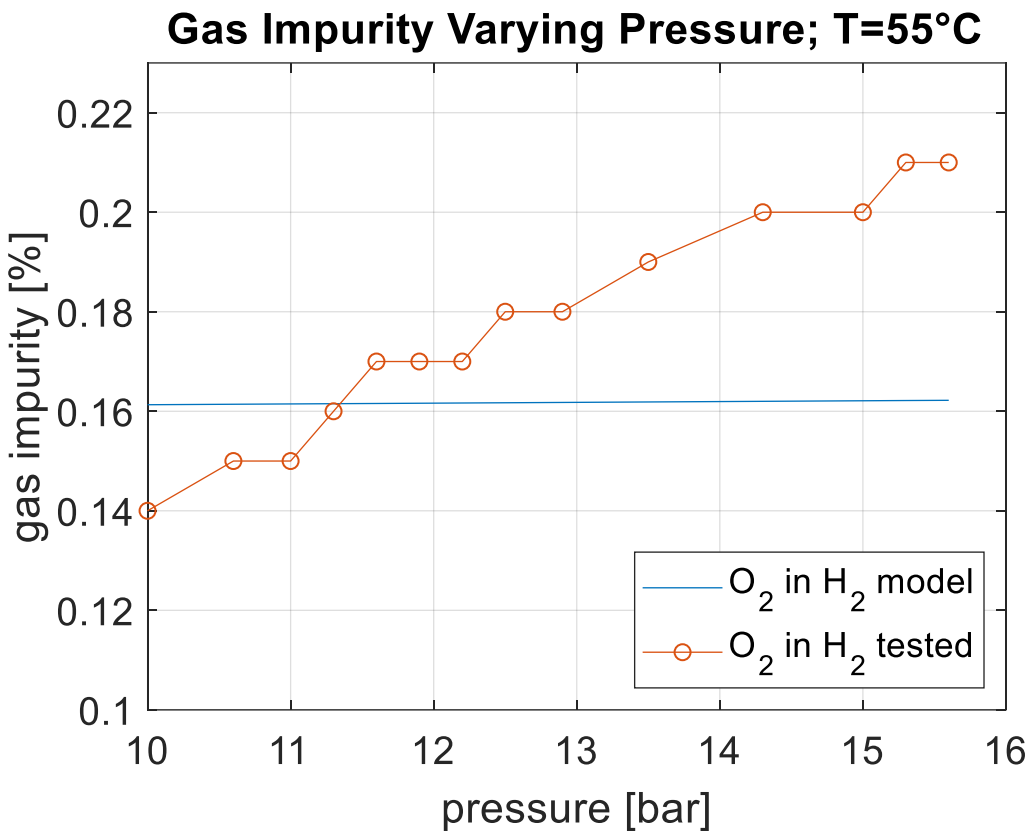

Fig. 5.2.2: Gas purity at T=55 °C

5.2.2 Case 2 – Inlet Power variation

With the study obtained before we know that the most important value for the outlet gas purity in the inlet power.

Accordingly, for the second case, the variation of inlet power is the parameter considered.

Case 2 – Test 1

For the first test, the value of inlet power from 22kW to 18kW has been changed.

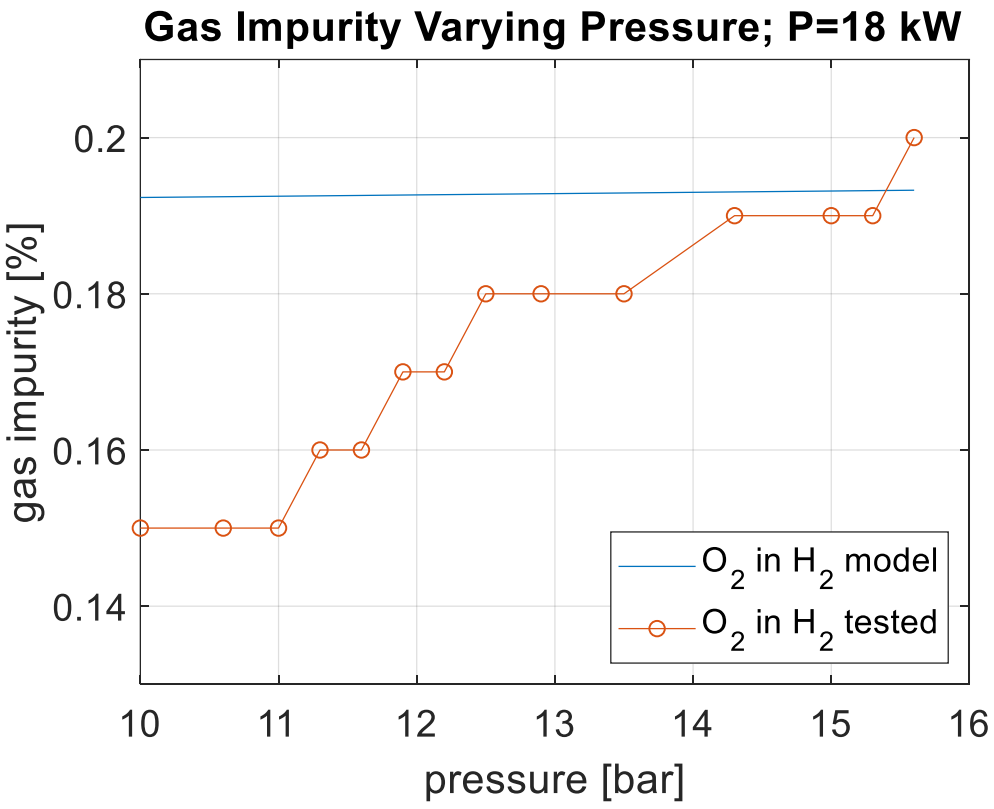

Fig. 5.2.3: Gas purity at P=18 kW

Case 2 – Test 2

For the second test, the value of inlet power from 22kW to 14kW has been changed.

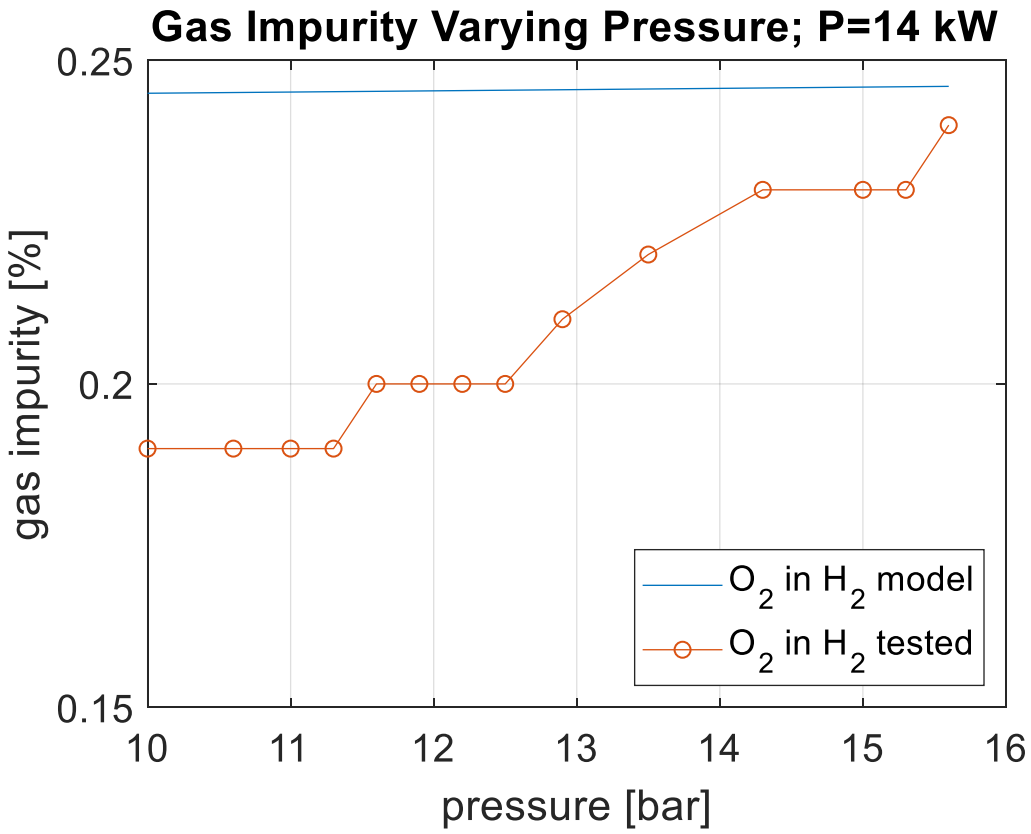

Fig. 5.2.4: Gas purity at P=14 kW

In the second case during tests the voltage was not constant like in the first case, so the results obtained from the model are considered in test 1 with V=65 V and in test 2 with V=60 V.

However, the case 2 – test 2 is the only one in which there is no intersection between model and experiment.

5.3 Comparison

At the end the figures shown below show the comparison between the different values of the model and the test at different conditions:

- The first figure showed the different value of outlet gas purity at a different value of temperature. As you can see the best solution is for T=65 °C that is the nominal operating value. For T=60 °C the results are similar, but it is not useful work at T=60 °C.

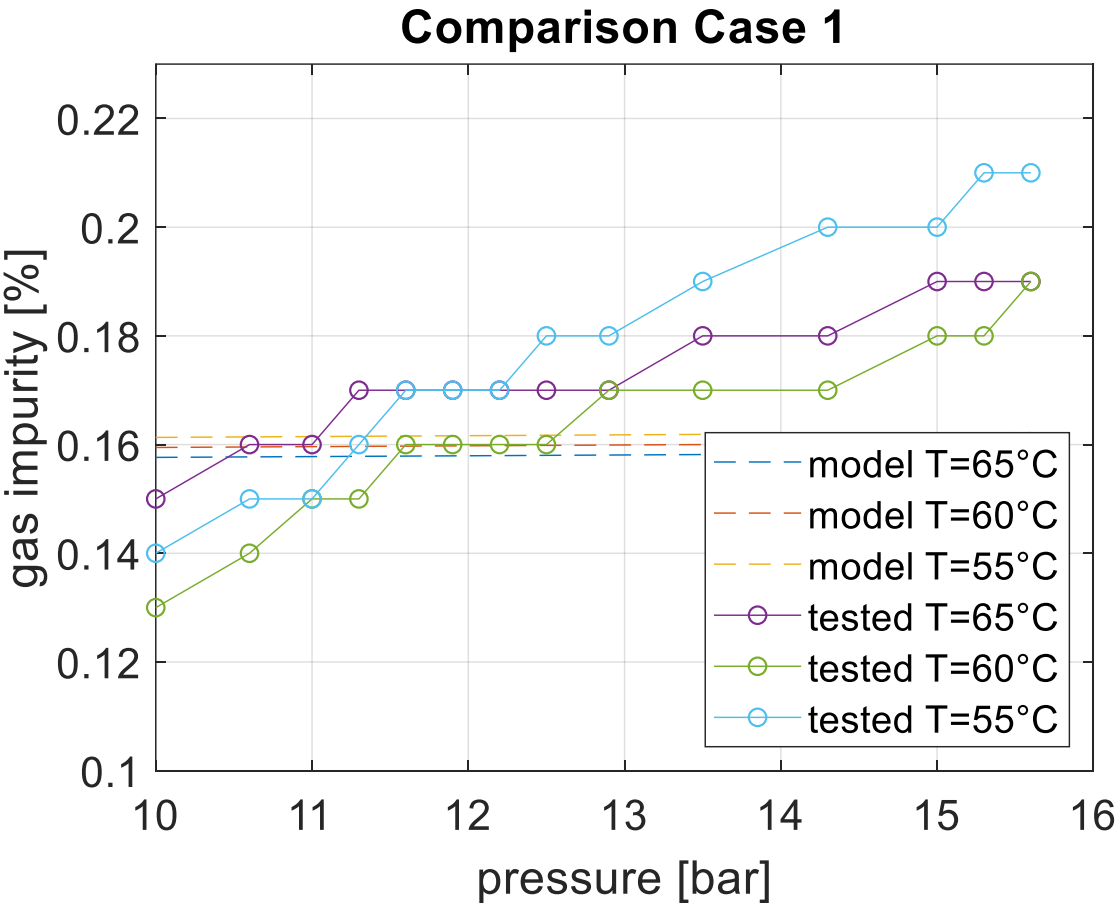

Fig. 5.3.1: Comparison between model and test at different value of the temperature

- The second figure showed the different value of outlet gas purity at a different value of inlet power. As expected the best solution is for P=22 kW that is the nominal operating value. For P=18 kW the results are similar, but it is not useful work at P=14 kW.

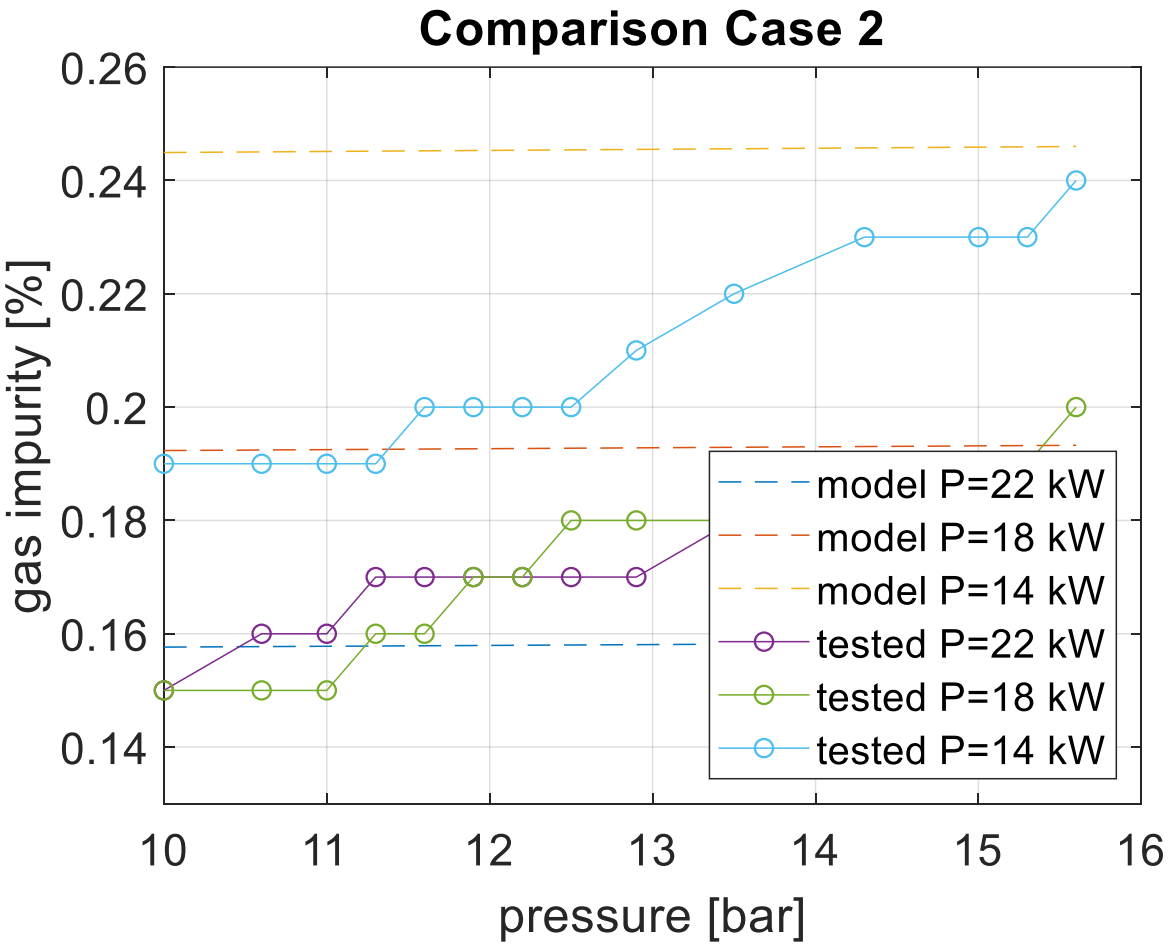

Fig. 5.3.2: Comparison between model and test at different value of inlet power.

6 Conclusions

Summarizing, the aim of this study was to estimate the hydrogen purity exhaust from the alkaline electrolyzer.

A theoretical model in Matlab scripts was build and several tests at E.EPS company were carried out.

The study performed has been useful to estimate which are the main parameters affecting the outlet gas purity.

Results obtained from the theoretical model are comparable to the ones from the literature.

Indeed, varying the current density, the percentage of hydrogen in oxygen at the anode is higher than the percentage of oxygen in hydrogen at the cathode and in both cases, the purity level decreases with the reduction of mass flow rate and KOH concentration.

Nevertheless, the electrolyte flow rate should be high to avoid the biggest amount of outlet gas flow rate.

The increase of KOH concentration from 30% to 32% gave improvements, and it can be changed to optimize the system works.

From the comparison of the theoretical model and the tests performed by the company, instead the results found are as expected: for high values of inlet power and the temperature the percentage of oxygen in hydrogen decreases.

So the current operating conditions are the best.

The future developments are several:

First of all, the theoretical model will be optimized by carrying out a sensitivity analysis to obtain the best values supposed in order to fit better the model's and test's results.

Mainly interest will be the slope of the line resulting from the model.

From the company's point of view, instead much more tests, applying another alkaline electrolyzer with different initial conditions, will be carried out: this AEC shall have the possibility of changing parameters like the inlet KOH concentration, due to the optimization given from the theoretical model, in order to do a comparison with the missing tests. This changing of the variable was not possible to do in Self 25.

It was also impracticable to obtain a comparison between 'mixed mode' and 'separated mode' because Self 25 works at 'mixed mode'.

From literature, the investigation reveals that gas purity in alkaline water electrolysis is mainly affected by mixing the anodic and cathodic electrolyte cycles, in fact in the 'separated mode' both cycles are separated from each other to prevent the contamination of the opposite product gas through gas dissolution.

Therefore, an economic analysis considering the gas purity, the power consumption, the efficiency and process management of an alkaline electrolyzer should be carried out for optimized operation.

References

[1] G. Giolito, «Experimental analysis and modeling of an alkaline electrolyzer + BoP for power-to-power applications».

[2] [Online]. Available: http://ec.europa.eu/research/participants/data/ref/h2020/other/legal/jtis/fch-multi-workplan_en.pdf.

[3] A. C. D. H. F. L. B. M. E. S. Luca Bertuccioli, «Study on development of water electrolysis in the EU, February 2014.».

[4] S. A. Savant, «ACCELERATED STRESS TESTING PROTOCOLS OF PROTON EXCHANGE MEMBRANE PEM ELECTROLYZERS».

[5] V. A. B. D. G. Minić, Hydrogen Economy: Modern Concepts, Challenges and Perspective.

[6] L. Y.-K. Lee W-J., «Internal Gas Pressure Charateristics Generated during Coal Carbonization in a Coke Oven,» *Energy & Fuels. - 2001.*.

[7] N. [. al.], «A review and recent developments in photocatalytic water-splitting using TiO2 for hydrogen production,» *Renewable and Sustainable Energy Reviews. - 2007.*.

[8] W. Y. H. Y. Z. Z. Tao Y. Chen Y., «High hydrogen yield from a two-step process of dark- and photo-fermentation of sucrose,» *International Journal of Hydrogen Energy. - 2007.*

[9] M. G. alga, « hydrogen production: progress, challenges and prospects,» *International Journal of Hydrogen Energy. - 2002.*.

[10] EPS, «Manual Self 25».

[11] B. K. M. K. T. T. Philipp Haug, «Process modelling of an alkaline water electrolyzer,» [Online].

[12] F. D. M. J. S. D. Carmo M, «A comprehensive review on PEM water electrolysis. Int J Hydrogen Energy 2013,» [Online]. Available: http://dx.doi.org/10.1016/j.ijhydene.2013.01.151.

[13] S. M. I. B. E. S. P. Ursua A, «Stand-alone operation of an alkaline water electrolyser fed by wind and photovoltaic systems.,» [Online]. Available: http://dx.doi.org/10.1016/j.ijhydene.2013.09.085..

[14] L. W. S. D. Schalenbach M, «Hydrogen diffusivity and electrolyte permeability of the Zirfon Perl separator for alkaline water electrolysis.,» [Online]. Available:

http://dx.doi.org/10.1149/2.1251613jes..

[15] [Online]. Available: Levenspiel O. Chemical reaction engineering. New Delhi:Wiley-India; 2012..

[16] D. O. D. J. Schillings J, «Modeling of electrochemically generated bubbly flow under buoyancy-driven and forced convection,» [Online]. Available: http://dx.doi.org/10.1016/j.ijheatmasstransfer.2015.01.121..

[17] V. H., «The role of single-phase free convection in mass transfer at gas evolving electrodes,» [Online]. Available: http://dx.doi.org/10.1016/0013-4686(93)80079-F..

[18] V. H. Eigeldinger J, «The bubble coverage of gas-evolving electrodes in a flowing electrolyte.,» [Online]. Available: http://dx.doi.org/10.1016/S0013-4686(00)00513-2.

[19] V. H., «The rate of gas evolution of electrodes,» [Online]. Available: http://dx.doi.org/10.1016/0013-4686(84)87043-7..

[20] N. S. T. Y. S. Y. O. Z. Kikuchi K, «Characteristics of hydrogen nanobubbles in solutions obtained with water electrolysis.,» [Online]. Available: http://dx.doi.org/10.1016/j.jelechem.2006.10.005..

[21] F. K., «Oberfl€achenspannung w€assriger NaOH- und KOH-L€osungen,» [Online]. Available: http://dx.doi.org/10.1002/cite.330412107..

[22] B. J., «Water vapour partial pressures and water activities in potassium and sodium hydroxide solutions over wide concentration and temperature ranges.,» [Online]. Available: http://dx.doi.org/10.1016/0360-3199(85)90093-X..

[23] K. G. V. S. W. t. R. A. Z. J. E.-H. R. Vogt H, «Electrochemical reactors.,» [Online]. Available: http://dx.doi.org/10.1002/14356007.l09_l01.pub2..

[24] V. H. Balzer RJ, «Effect of electrolyte flow on the bubble coverage of vertical gas-evolving electrodes.,» [Online]. Available: http://dx.doi.org/10.1149/1.1524185..

[25] V. H., «On the gas-evolution efficiency of electrodes I - theoretical.,» [Online]. Available: http://dx.doi.org/10.1016/j.electacta.2010.08.101..

[26] [Online]. Available: Wesselingh JA, Krishna R. Mass transfer in multicomponent mixtures. Delft: VSSD; 2006..

[27] [Online]. Available: Levenspiel O. Chemical reaction engineering. New Delhi: Wiley-India; 2012..

[28] H. DM.. [Online]. Available: http://dx.doi.org/10.1021/je60005a003..

[29] S. A. Weisenberger S, «Estimation of gas solubilities in salt solutions at temperatures from 273 K to 363 K.,» [Online]. Available: http://dx.doi.org/10.1002/aic.690420130.

[30] [Online]. Available: Knaster MB, Apel'baum LA. Solubility of hydrogen and oxygen in concentrated potassium hydroxide solution. Russ J Phys Chem 1964;38:120e2..

[31] M. D. Brauer H, «Str€omungswiderstand sowie station€arer Stoff- und W€armeu¨ bergang an Blasen und Tropfen.,» [Online]. Available: http://dx.doi.org/10.1002/cite.330441513.

[32] [Online]. Available: Peebles FN, Garber HJ. Studies on the motion of gas bubbles in liquids. Chem Eng Prog 1953;49(2):88e97..

[33] [Online]. Available: Grassmann P. Physikalische Grundlagen derVerfahrenstechnik. Sauerl€ander Frankfurt/Main. 1970..

[34] [Online]. Available: Kienzlen V. Potentialverteilung an gasentwickelnden Elektroden. In: Institut fu¨ r Technische Thermodynamik. DLR Forschungsbericht; 1992..

[35] K. M. Kreysa G, «Modelling of gas evolving electrolysis cells. I.,» [Online]. Available: http://dx.doi.org/10.1007/BF01059293..

[36] T. H. Brauer H, «Bewegung von Partikelschw€armen.,» [Online]. Available: http://dx.doi.org/10.1002/cite.330451317..

[37] M. P. Guillet N, «Alkaline water electrolysis.,» [Online]. Available: http://dx.doi.org/10.1002/9783527676507.ch4..

[38] B. B. R. S. H.-R. R. K. Trinke P, «Hydrogen permeation in PEM electrolyzer cells operated at asymmetric pressure conditions.,» [Online]. Available: http://dx.doi.org/10.1149/2.0221611jes..

[39] W. R. G. K. Tham MK, «Diffusion of oxygen and hydrogen in aqueous potassium.,» [Online]. Available: http://dx.doi.org/10.1021/j100703a015..

[40] V. H., «Mechanisms of mass transfer of dissolved gas from a gas-evolving electrode and their effect on mass transfer coefficient and concentration overpotential.,» [Online]. Available: http://dx.doi.org/10.1007/BF01320646..

[41] K. M. T. T. Haug P, «Influence of process conditions on gas purity in alkaline water electrolysis.,» [Online].

[42] J. L. v. S. S. V. J. W. Chin Kwie Joe JM, «Bubble parameters and efficiency of gas bubble evolution for a chlorine-, a hydrogen- and an oxygen evolving wire electrode.,» [Online]. Available:

http://dx.doi.org/10.1016/S0013-4686(98)80006-6..

[43] B. R. Vogt H, «The bubble coverage of gas-evolving electrodes in stagnant electrolytes.,» [Online]. Available: http://dx.doi.org/10.1016/j.electacta.2004.09.025..

[44] D. O. Sigrist L, «On the conductivity and void fraction of gas dispersions in electrolyte solutions.,» [Online]. Available: http://dx.doi.org/10.1007/BF00726089.

[45] Fuel Cells and Hydrogen Joint Undertaking (FCH JU), « Multi Annual Work Plan 2014-2020, background chapter.».

[46] [Online]. Available: Wesselingh JA, Krishna R. Mass transfer in multicomponent mixtures. Delft: VSSD; 2006..